

# Mechanical Behavior of Aluminum- Graphene Composite as a Result of Thermo-Mechanical Treatment

*Submitted in the partial fulfillment of the requirement for the  
award of the degree*

*Of*

**MASTER OF TECHNOLOGY**

**In Industrial Metallurgy**

*Under the supervision of Dr. Debrupa Lahiri*

**Jijo ChristudasJustus | M.Tech. Project Thesis | 17<sup>th</sup> May, 2018**



## CANDIDATE'S DECLARATION

I hereby declare that the proposed work presented in this dissertation entitled “**Mechanical Behavior of Aluminum-Graphene as a Result of Thermo-Mechanical Treatment**” is in partial fulfilment of the requirements for the award of the degree of **Master of Technology in Industrial Metallurgy**, submitted in the **Department of Metallurgical and Materials Engineering, Indian Institute of Technology Roorkee** is an authentic record of my own work carried out during the period of July 2017 to May 2018 under the supervision of **Dr. Debrupa Lahiri**, Assistant Professor, Department of Metallurgical and Materials Engineering, Indian Institute of Technology Roorkee, India.

The matter presented in this dissertation has not been submitted by me for the award of any other degree.

Dated: 17<sup>th</sup> May, 2018

Place: Roorkee

(Jijo ChristudasJustus)

## CERTIFICATE

This is to certify that the above statement made by the candidate is correct to the best of my knowledge and belief

Dr. Debrupa Lahiri

Assistant Professor

Metallurgical and Materials Engineering

Indian Institute of Technology-Roorkee

Roorkee-247667 (India)

## ACKNOWLEDGEMENT

I owe a great many thanks to a great many people who helped and supported me during writing of this thesis.

My deepest thanks to my advisor Dr. Debrupa Lahiri (Assistant Professor, IIT Roorkee) who guided me and corrected my various mistakes with attention and care. She has taken pain to go through the project and make necessary corrections as and when needed.

I express my thanks to the HOD of Department of Metallurgical and Materials Engineering Dr Anjan Sil for his precious support.

My deep sense of gratitude to my colleagues and lab members Miss Ankita Bisht, Mr. Satish Jaiswal, and Miss Anshu Dubey for their support, encouragement, guidance and for reviewing my work.

I would also thank my Institution and all the professors of Department without whom this project would have been a distant reality. I also extend my heartfelt thanks to my well-wishers.

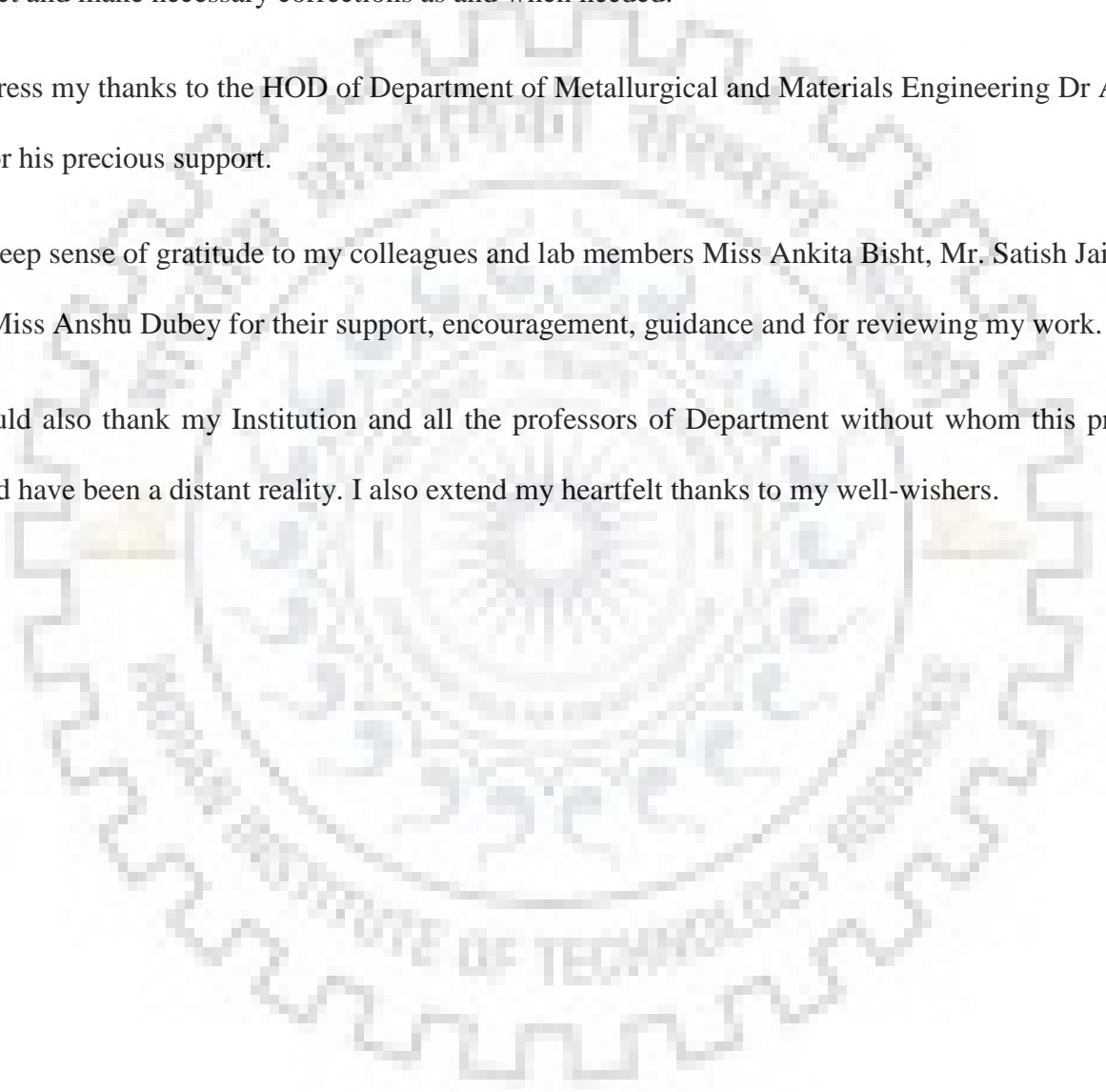


## TABLE OF CONTENTS

<b>ABSTRACT</b> .....	vii
<b>1. INTRODUCTION</b> .....	2
1.1 WHY ALUMINUM? .....	3
1.1.1 Aircraft .....	3
1.1.2 Electrical Conductors .....	4
1.1.3 Packaging.....	4
1.1.4 Building and Architecture.....	4
1.2 GRAPHENE.....	5
<b>2. LITERATURE REVIEW</b> .....	8
2.1 IMPORTANCE OF MATERIAL AND PROCESSING ROUTE.....	8
2.1.1 Importance of Metal- Graphene Composite.....	8
2.1.2 Importance of Aluminum –Carbon Composite.....	13
2.2 IMPORTANCE OF SPARK PLASMA SINTERING .....	17
<b>3. OBJECTIVES AND PLAN OF WORK</b> .....	21
3.1 OBJECTIVES OF WORK .....	21
3.2 METHODOLOGY .....	22
<b>4. MATERIALS AND METHODS</b> .....	24
4.1 FABRICATION OF COMPOSITES .....	25
4.2 MECHANICAL AND STRUCTURAL ANALYSIS.....	26
<b>5. RESULTS AND DISCUSSIONS</b> .....	30
5.1 MORPHOLOGY OF GNP/AL COMPOSITES.....	30
5.2 STRUCTURAL CHARACTERIZATION OF GNP POWDER AND GNP/AL COMPOSITE.....	36
5.3 MECHANICAL BEHAVIOR OF COMPOSITES.....	37
<b>6. CONCLUSION</b> .....	42
<b>LIST OF CONFERENCE PRESENTATION</b> .....	43
<b>REFERENCES</b> .....	44

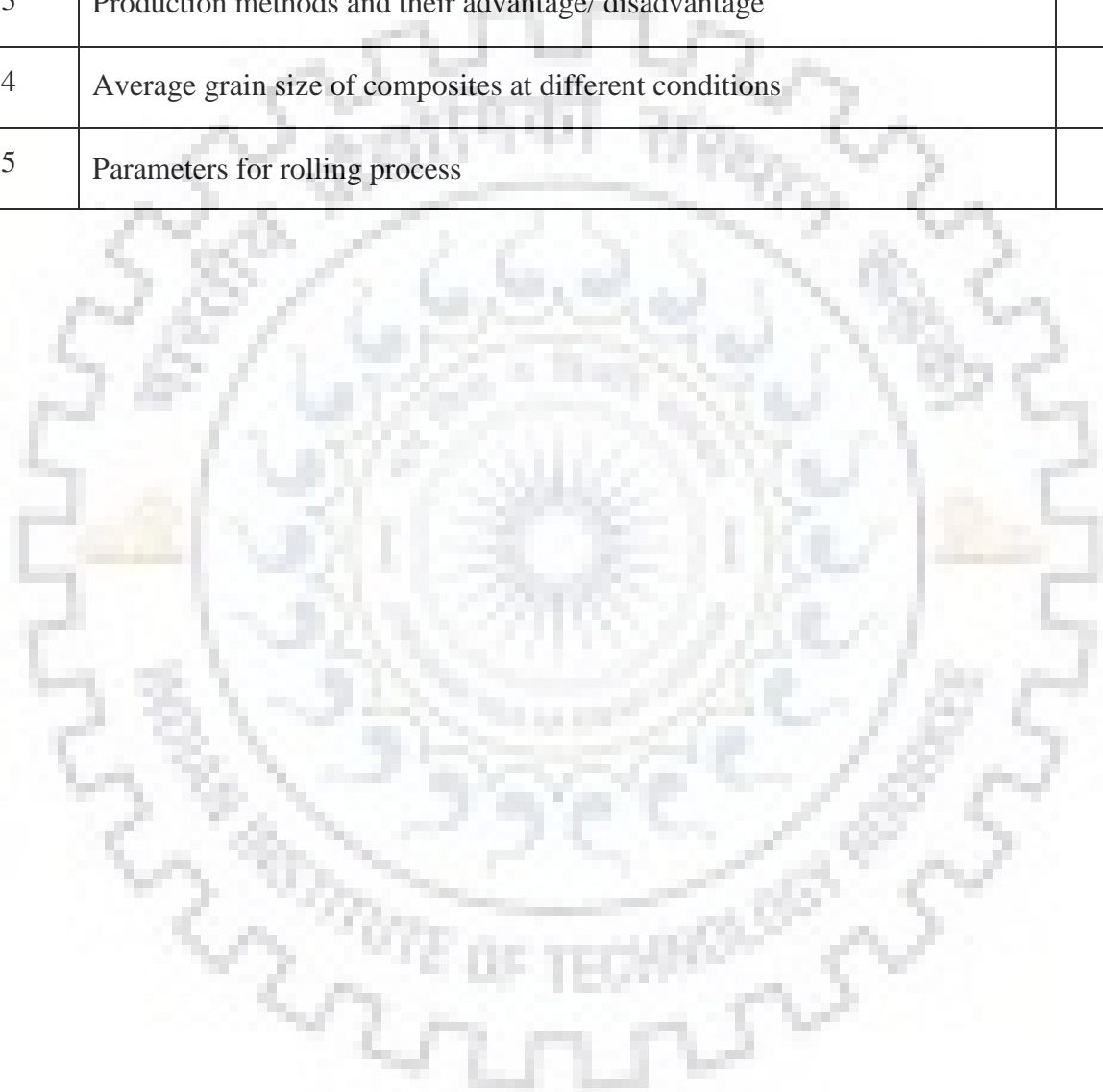
## LIST OF FIGURES

Fig. No.	Title	Page
1	(a) TEM image of Al-1wt% GNF composite, (b)TEM image of Al-0.5 wt% GNF and (c) Tensile properties verses the weight fraction	10
2	(a) Typical compressive strength curves of the sintered composites with different graphene contents, (b) Bright field TEM image of laminated graphene plates	11
3	(a) TEM images of GNSs/Al composites Al-0.25 GNSs, (b) The variation tendencies of yield strength and ultimate tensile strength with GNSs content	12
4	Variation of (b) ultimate tensile and yield strength and (c) ductility for pure Al and GNP/Al composite structures	13
5	Graph of true stress-strain for the cold-rolled samples under (a) Tensile testing at different temperatures with the same strain rate, (b) at 400°C, (c)(d) Plot of elongation to failure vs temperature (white column) and corresponding strain at which the maximum stress is reached (gray column)	16
6	Stress vs strain curve	16
7	Compression tests results for the pure Al bar and the Al/GO and Al/CNT composites. (a) Typical engineering stress–engineering strain curves. The inset shows the corresponding normalized work hardening rate curves, (b) Average engineering stress at 5, 15 and 25% engineering strain	17
8	SEM images of (a) Al, (b) GNP	24
9	Process for mixing the Al and GNP powder	24

10	(a) Layout of the SPS inner chamber and (b) Prepared sample from SPS	25
11	Section cut for tensile test	27
12	Hysitron TI-950 Triboindenter	27
13	SEM image of 0.75GNP/Al powder	30
14	Optical microscopy of (a)(d)(g)(j) Pure Al, (b)(e)(h)(k) 0.5GNP/Al and (c)(f)(i)(l) 0.75GNP/Al for As-Sintered, RR, WR and RA condition, respectively	31
15	EDS mapping of (a) 0.5GNP/Al and (b) 0.75GNP/Al	33
16	SEM micrographs of (a)(d)(g)(j) Pure Al, (b)(e)(h)(k) 0.5GNP/Al and (c)(f)(i)(l) 0.75GNP/Al for As-Sintered, RR, WR and RA condition, respectively. Voids are indicated by arrows while GNP with dotted circles	34
17	TEM images of 0.5GNP/Al (a), (b) As-sintered and (c), (d) RR	35
18	XRD graph for Pure Al, Pure GNP and GNP/Al	36
19	Tensile stress-strain curve of (a) As Sintered, (b) RR, (c) WR and (d) RA for different composites	37
20	Variation of (a) Ultimate Tensile Strength, (b) Yield Strength, (c) Toughness and (d) Ductility of different composites for as-sintered, RR, WR and RA conditions	38
21	Representation of load vs. depth curve obtained from nano-indentation tests of (a) As-sintered, (b) RR, (c) WR, (d) RA; Variation in (e) hardness and (f) Elastic modulus	39

## LIST OF TABLES

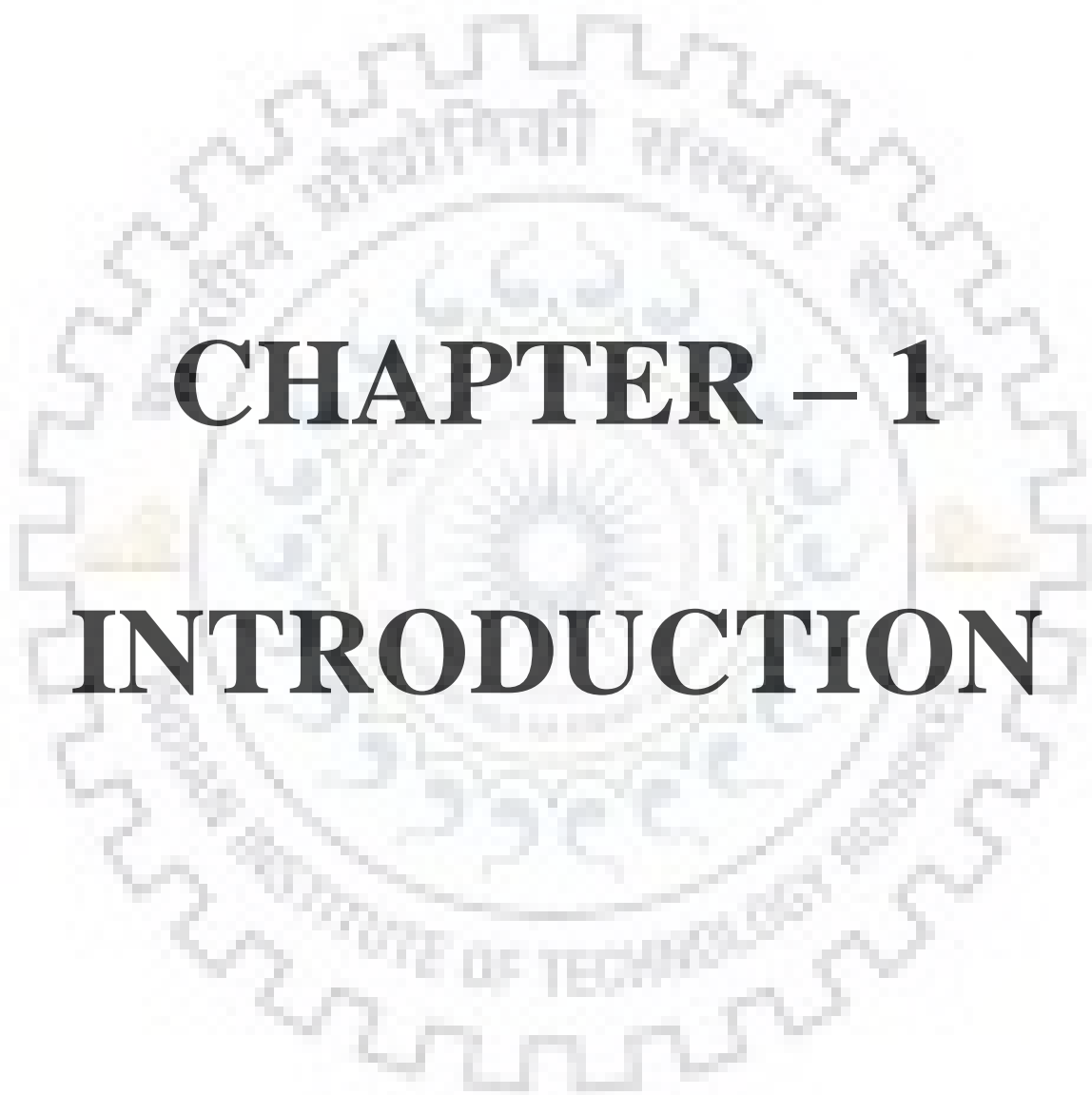
Table No.	Title	Page
1	Metal Graphene composite and its application	10
2	Carbon Aluminum composite and their processing route	14
3	Production methods and their advantage/ disadvantage	18
4	Average grain size of composites at different conditions	31
5	Parameters for rolling process	31



## ABSTRACT

With all the superlative properties, like, high strength to weight ratio, fracture strength, Young's modulus, good thermal and electrical property, graphene has held the desirability for the replacement with the existing materials in the field of aerospace, electronics and automobiles. Thus, graphene is a potential candidate to be used as reinforcement in light weight metal matrix composite, like aluminum. In the present study, aluminum matrix composite, with varied composition of graphene nano-platelets (GNP), was synthesized by spark plasma sintering to near theoretical densities. They were further analyzed by X-Ray diffraction to detect presence of any oxides or carbides during consolidation. It is seen that addition of GNP upto some extent is improving the strength and hardness of the material. These composites were further cold rolled and warm rolled (i.e. at 250°C) by thermo-mechanical processing (TMP) to examine the change in properties. The microstructural evolution, taking place under severe plastic deformation, is analyzed. The change in the mechanical properties of Al/GNP due to the effect of rolling strain and temperature, is evaluated by tensile testing and nano-indentation measurements. The main reasons stimulating grain refinement at this temperature and the relative contribution of different strengthening effect is analyzed in detail.





# **CHAPTER – 1**

# **INTRODUCTION**

## 1. INTRODUCTION

Metal-matrix nanocomposites represent advanced materials that are highly attractive for a wide range of structural and functional applications. Indeed, modification of the microstructure of metallic materials by nanoscale inclusions can effectively enhance and control various properties of these materials. To satisfy the needs of engineering application, in most cases, the tensile strain is required to be 7-8% at least in the structural materials [1]. Above all, the engineering applications of the nanostructured AMCs is mostly limited due to the poor combination of strength and ductility. In recent years, a rapidly growing attention has been noted for graphene (Gr), that exhibit unique combination of electronic, mechanical, and thermal properties and thereby are of utmost interest for use as fillers in metal-matrix composites. With superior mechanical properties (strength ~130 GPa, Young modulus ~1 TPa) of graphene [2], it serves as excellent strengthening inclusions in metal-matrix composites.

Among metal-graphene nanocomposites, Al/Gr composites have attracted a special attention due to low weight of aluminum, coupled with its high specific strength and good ductility. Insertion of graphene nano inclusions into Al-matrix significantly increases both hardness and fracture strength [2]. At the same time, plasticity of Al/Gr composites is rather poor. Carbon nano-tube-reinforced aluminum composites (CNT/Al) have been researched greatly over the past decade, to meet the increasing needs for structural strength and energy efficiency. Even though, several developments have been made, it may still be delayed until Al/CNT composites are used in practical applications. The main task is to get CNTs to disperse homogeneously in the Al matrix, avoiding the structure of CNTs being damaged. Compared with CNTs, graphene is easier to handle and disperse in solvents or all kinds of matrices. Therefore, it is evident that Al/Gr has a good potential to replace Al/CNT as a candidate for the next-generation MMCs [3].

## 1.1 WHY ALUMINUM?

### 1.1.1 Aircraft

The writer Jules Verne was the former person to emphasize the prospective of aluminum in the aerospace industry. His novel named *Journey to the Moon* mentioned a comprehensive description of an Al rocket. During 1903, using aluminum crankcase engine, the Wright brothers made their wood-framed biplane. In WWI, lightweight aluminum became crucial in aircraft improvement and design. During WWII, the fabrication of aluminum ascended. U.S. aircraft manufacturing (1940-1945) totaled an amazing 296,000 aircraft. Primarily, more than 50% were prepared from aluminum. From there, alloys were used to build initial rockets. Al alloys were used to fabricate the body casting of the Titan rockets and the Avantgarde used for launching into orbit the first American rockets.

Aluminum appears to be the king of aircraft structure, though in latest years some new Al alloys have been applied. These super alloys are still relatively costly for the aircraft builders. With its good strength to weight and cost ratio, aluminum still widely used in the industries. The airframe of a distinctive modern commercial carriage aircraft is 80wt% aluminum. Aluminum alloys are the irresistible choice for the wing, fuselage, military cargo/transport aircraft and supporting structures of commercial airliners. Wrought aluminum is used for the manufacturing of structural components of current United States Navy aircraft. Aluminum has been the optimal material for space structures, ever since the launch of Sputnik occurred half-century ago. Aluminum alloys reliably surpass other metals in such areas as thermal management, mechanical stability, damping and light weight. Because of its light weight and its ability to endure the stresses that happen during operation and launch in space, aluminum has been used on the space shuttles, Apollo spacecraft, the Skylab, the International Space Station, etc.

### 1.1.2 Electrical Conductors

Even in domestic wiring, 6000 or 1000 series Al alloys for electrical conductors are sensible technical replacements to copper. Aluminum is used rather than copper for very great amount of overhead, high voltage, power lines as the conductor on weight grounds. According to the International Annealed Copper Standard (IACS), aluminum alloys have an average conductivity of 62% but, due to its density, it can carry twice as much current as compared to copper weight.

### 1.1.3 Packaging

The 1000 Al series is used as foil for the purpose of food wrapping and for containers due to its resistance against corrosion and barrier properties against UV light, odor and moisture. If required, as foil can be easily formed, it can be used for decorating and combined with plastic and papers. The most important use of aluminum in packing has been in the manufacturing of beverage cans that include the 'easy open ring pull' on the lid. This has boosted the rapid growth to approx. 15% of aluminum use. Cans is also used for preserving food products like fish, employs the cool opening facilities due to aluminum.

### 1.1.4 Building and Architecture

For the application like building and construction, aluminum is used for a wide range. These consist of roofing for factories that include foil vapor barriers, windows and pre formed sheet cladding features, architectural hardware and fittings, doors, canopies and fronts for shops and impressive buildings, replacement windows and rainwater goods. Aluminum structures and cladding are also used to renovate numerous of the concrete structures built in the 1950-60's that are now showing signs of weakening and spoiling.

Aluminum is of supreme significance in terms of durability for construction applications. There are numerous of examples for the durability of aluminum that may be familiar which includes the statue of Eros situated in Picadilly Circus, London erected in 1893 and the clad dome of the church of San Gioacchino situated in Rome that was installed in 1887. Recently, aluminum is widely used in the oil and gas industry for offshore structures. The 6000, 5000, 3000, 1000 and wrought series Al alloys has shown no deterioration of strength having no protection even in marine and industrial environments. However, it is advisable to paint or anodize to preserve the appearance and protection to some extent.

Many researches are dedicated to find the better choice for metal matrix for Graphene reinforcement. Many metals shows very good improvement compare to their base metal. But still in structural application like aerospace, automobile etc. high strength to weight ratio is required. Many researches has done on metal matrix graphene reinforced composite for structural application such copper, nickel [4], aluminum [5], magnesium [6], and titanium [7]. As we know, magnesium has lowest density among all metals. Although, it facilitates excellent damping properties, excellent castability and large abundance, it lacks in some properties like it has low corrosion resistance, mechanical strength and poor creep. Due to these limitations, magnesium applications are also limited in structural applications. Titanium can also be another choice due to their good properties but its thermal conductivity is less than others due to which at relatively higher temperature thermal stresses can be induced which restricts the use of titanium in some areas. Copper and nickel has comparatively higher density which results in low strength to weight ratio in comparison to aluminum which makes aluminum, an appropriate choice for matrix material. Aluminum has good corrosion resistance, high strength to weight ratio, high thermal conductivity and good forming ability [6].

## 1.2 GRAPHENE

Graphite is an allotropic form of carbon which is abundant in nature. It consist of atomic layers of covalently bonded  $sp^2$  hybridized carbon and these layers are stacked by weak vander waals forces.

Single layer of carbon atoms of honeycomb structure is called graphene. It has mechanical properties (strength~130 GPa, elastic modulus~1,002 GPa, thermal conductivity~4840-5350 Wm<sup>-1</sup> K<sup>-1</sup> and coefficient of thermal expansion -1.3E-6) [6][8]. Graphene[9]–[13] was found far better than graphite in many aspects like electronic conductivity and mechanical properties. In 2010, Andre Geim and Konstantin Novoselov was awarded by Noble prize for discovery of graphene by scotch tape method. There are two type of approaches was followed by researchers for production of graphene, one is top down and another one is bottom up approach. In top down approach particle size will be reduce upto our desired size (e.g. Exfoliation of graphite to get monolayer or multilayer graphene) while in bottom-up approach particle size will be increase upto desired size. In the context, it can be said that graphene electrical or mechanical property totally depends on graphene structure which can only be decided by the approach for production of graphene [14][15]. Graphene as a reinforcing agent [1], [5], [16]–[23] has emerged to have better interfacial bonding with matrix due to its high surface area. Single layer graphene is expensive and difficult to isolate. Whereas, GNP, used here for the study, comprises of few number of graphene layers holding comparable properties to that of single layer graphene; in fact, much easier to produce and handle [24][3]. These sheets of graphene in GNPs are bonded with each other by van der waals force and possess the spring constant of 1-5 N/m [25].

In order to improve the mechanical properties by microstructural refinement, various approaches has been designed for e.g. powder metallurgy [26], spray forming [27], low frequency electromagnetic casting [28], severe plastic deformation (SPD) which includes accumulative roll bonding (ARB) [29], equal channel angular pressing (ECAP) [30], multi direction forging (MDF) [31], cryogenic rolling (CR) [32] and thermo-mechanical processing (TMP) [33]. Thermo-mechanical processing (TMP) is still industrially preferred for grain refinement of Al alloys as it has simple process flow, high performance to cost ratio, large scale and continuous production efficiency which is a significant advantage over ARB, ECAP and CR techniques[34].



**CHAPTER – 2**

**LITERATURE  
REVIEW**

## 2. LITERATURE REVIEW

### 2.1 IMPORTANCE OF MATERIAL AND PROCESSING ROUTE

#### 2.1.1 Importance of Metal- Graphene Composite

There are many areas for which graphene – metal composite are developed, like, electrical, structural, biomedical applications. As far as structural applications are concerned, graphene is used as a reinforcement because of its outstanding mechanical properties and unique structure. But, still we have to look for many aspects, such as dispersion technique- proper dispersion is difficult, density difference between graphene-metal and interfacial area being more compare to other carbon material (carbon fibers, CNT etc.).

In the present scenario, graphene oxide and graphene are attracting researchers due to their uniqueness in mechanical properties. Dispersion of GNPs in metals are presently done by chemical mixing and mechanical mixing. In chemical mixing GNPs are first mixed with metal by mechanical agitator.. While, in mechanical mixing, Graphene oxide (GO) and GNP is first exfoliated in several nano-sheets and it is followed by ball milling. Uniform dispersion of GNPs in metal is first and the foremost requirement for good properties. Powder metallurgy is most popular solid state method for metal matrix composite. In this method, matrix and reinforcement are properly blended with each other with one of any above mention methods and compressed in molds. After that, at last stage, sintering is required to bond its metallic particle and reinforcement to increase strength and hardness. In case of Al/GNP composite, there is significant difference in coefficient of thermal expansion between aluminum and GNP, which creates high dislocation density at the interface of Al/GNP interface. This plays an important role in strengthening of composite. After that, during hot extrusion and rolling, GNPs are align in a particular direction and act as barrier for dislocation propagation [35].



Table 1: Metal Graphene composite and its application

Composition of composites	Properties and applications	Ref
Pt- Graphene	Act as a Super capacitor in fuel cell application	[36]
Al/Pd/Pt/Au Graphene	Bio medical application	[37][38][39]
Co/Si-Graphene	Act as anode material in Li-ion Battery applications	[40]
Al-Graphene	Graphene act as a reinforcing agent increase strength and hardness	[5]
Mg-Graphene	Ultra high strength	[41]
Cu graphene	Increase in electrical conductivity and hardness from base material	[42]

Cryo-milling was used for mixing of Aluminum-GNF powder. This improved metallurgical interface between them as good interface is an essential requirement for stress transfer. With an addition of

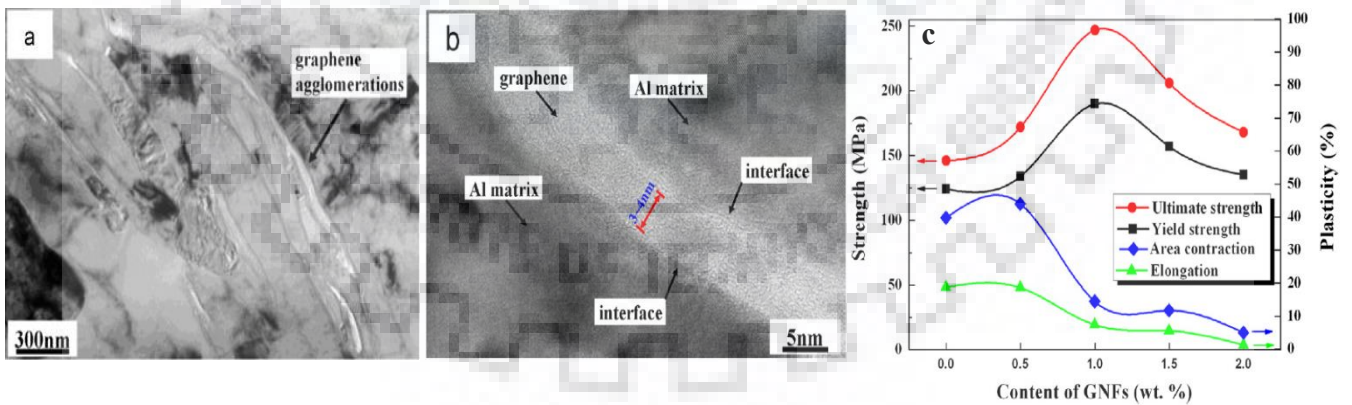


Fig. 1 (a) TEM image of Al-1wt% GNF composite, (b)TEM image of Al- 0.5 wt% GNF and (c) Tensile properties versus the weight fraction [16]

1wt% GNF, tensile strength and 0.2% offset yield strength increased by 68.7% and 55.2%, respectively, with decrease in ductility by 52% as shown in Fig. 1(c). The agglomeration of GNFs at

the grain boundary of aluminum in bright field TEM image is observed in fig. 1(a and b). which reduces the ductility, but formation of  $Al_4C_3$  was not observed. But strength increases due to agglomeration of GNF which itself gave the reinforcing effect. Increasing GNF content more than 1 wt% led to poor dispersion which ultimately led to reduce strength and ductility [1].

7055 aluminum alloy powder with a diameter of  $50\mu m$  was used as the metal matrix material. The graphene plates were chemically reduced from graphene oxide (GO) suspension by hydrazine, and the GO was prepared via the Hummer's method. The spark plasma sintering method was adopted at  $400^\circ C$  in vacuum with a 1 min dwell time and a heating rate of  $50^\circ C/min$ . A uniaxial pressure of 50 MPa was applied during the whole SPS process. The yield strength and compressive strength increased by 34.9% and 22.1%, respectively with 1wt%Gr, compared to pure 7055 aluminum alloy as shown in Fig. 2(a). This was reasoned as the strengthening effect attributed by the super-high strength of graphene and the homogeneous dispersion in the alloy matrix. Graphene plates inhibited the grain growth by grain boundary pinning. The graphene and metal matrix also exhibited clean and strong interfaces (fig. 2(b)). Moreover, detrimental aluminum carbide ( $Al_4C_3$ ) was not formed during SPS processing because of the low sintering temperature and non-milling blending process. Further addition of graphene (3wt%

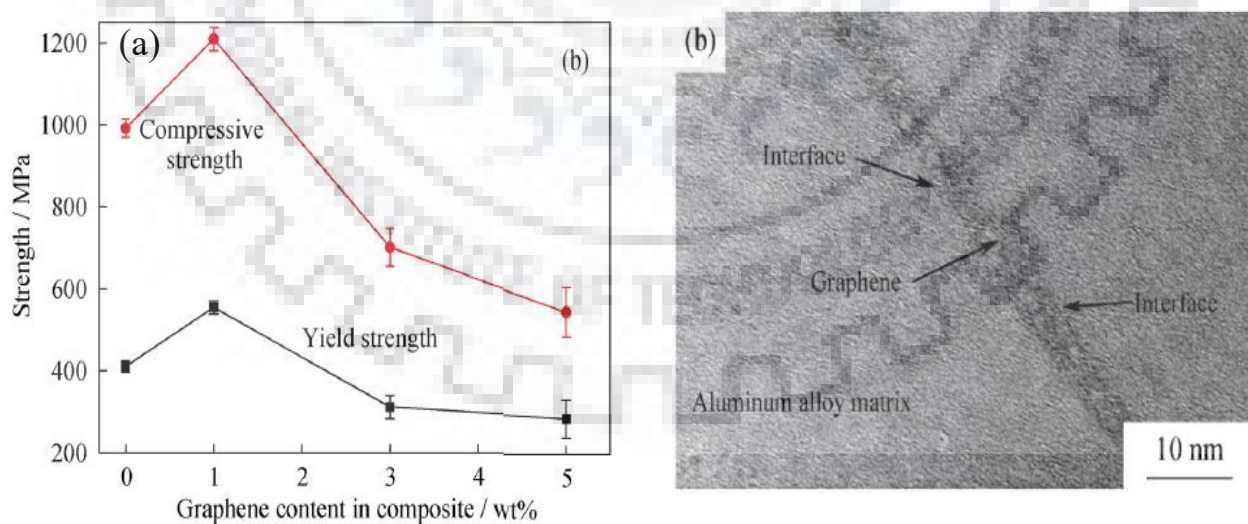


Fig. 2 (a) Typical compressive strength curves of the sintered composites with different graphene contents, (b) Bright field TEM image of laminated graphene plates [43]

and 5wt%) deteriorated the mechanical properties of the composites owing to the agglomeration of graphene plates [43].

Maximum enhancement of ultimate tensile strength and yield strength in 0.25wt%GNSs/Al compared to that of pure Al indicating the enhancement by 56.19% and 38.27%, respectively is seen in Fig. 3 (b). The GNSs/Al composites having relative density of 99.0% were prepared by high-energy ball milling and vacuum hot pressing. The GNSs were claimed to be distributed homogeneously throughout matrix. A clean interfacial bonding were obtained in GNSs/Al composites. The  $Al_4C_3$  (aluminum carbide) phases with short rod-like and granular morphology were observed at interface (fig. 3(a)). The GNSs pull-out was noticed at the edges of dimples, and the number of dimples slightly reduces with the increment of *GNSs content* [44].

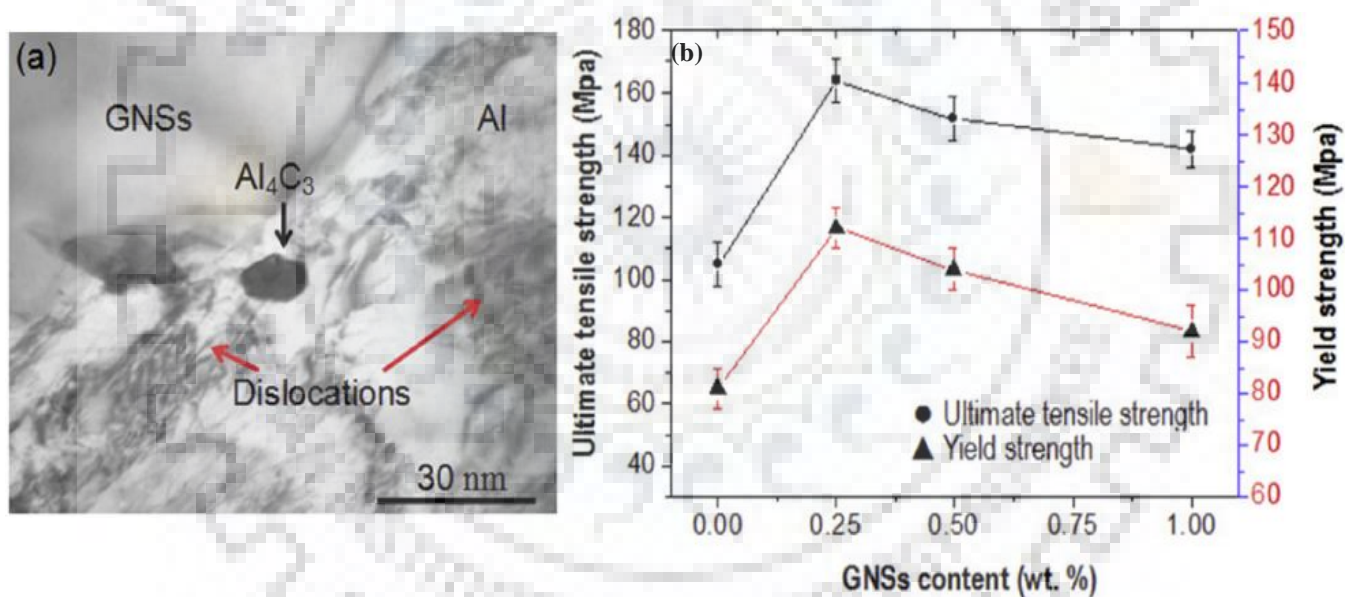


Fig. 3 (a) TEM images of 0.25wt% GNSs/Al, (b) The variation tendencies of ultimate tensile strength and yield strength with GNSs content [44]

GNP/Al upto 5wt% GNP content, were manufactured by SPS. Composite strength was seen to be dependent upon the homogenous dispersion and content of GNP in Al matrix. Reaction product like  $Al_4C_3$  was not found at GNP/Al interface in noteworthy amount when examined by X-ray diffraction. With 1wt% GNP, nano-indentation test revealed enhancement of 21.4% in hardness. High resistance to matrix was provided against deformation due to the presence of GNP. With 1wt% GNP,

enhancement in tensile strength and yield strength was 54.8% and 84.5%, respectively. At higher concentration, mechanical properties was degraded as a result of GNP agglomeration. Composite strengthening due to reinforcing effect of GNP was seen to be subjected by Orowan strengthening mechanism. Due to pinning effect of GNP, there was a homogenous distribution in grain size in the composite. Generally, GNP reinforcement has presented 86% enhancement in specific strength of Al matrix [45]. Also, no  $Al_4C_3$  phase was detected in GNP reinforced pure Al composites fabricated by the pressure infiltration method [46].

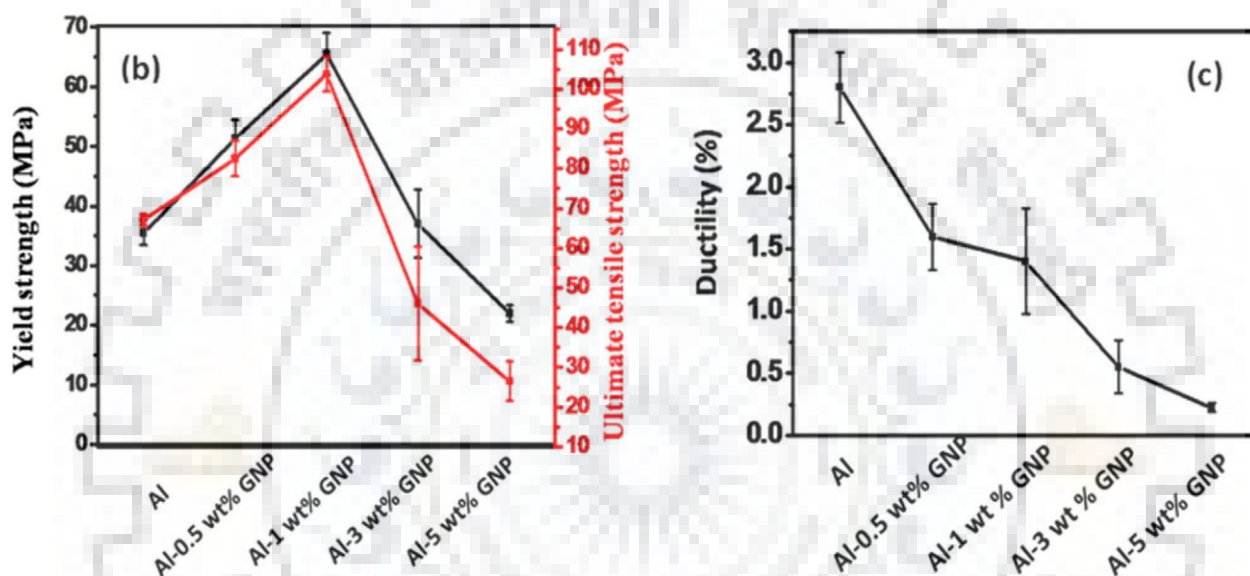


Fig. 4 Variation of (b) ultimate tensile and yield strength and (c) ductility for pure Al and GNP/Al composite structures[45]

GNP/Al composite upto 0.2wt% reinforcement content was prepared by ball milling and followed by cold pressing. Several micro-cracks were seen at the interface of GNP and Al which led to the decrement of ductility of the material. The UTS of 0.2wt%GNP/Al was approx. 36.8% more compared to pure Al with the same casting and rolling process [47].

Graphene reinforced aluminum matrix composites (Gr/Al) prepared by ball milling and followed by laser 3D printing was also seen to have the presence of  $Al_4C_3$  [48]. In another paper, GNP/Al composite having 0.4 wt% and 2.0 wt% reinforcing content were prepared by powder metallurgy followed by cold drawing with multi-pass to reduce the GNP agglomeration. The as-drawn 0.4 wt% GNP/Al



composites was showing 52% more ultimate tensile strength compared to Al alloy due to strong interfacial bonding. Whereas, 2wt% GNP/Al deteriorated in terms of mechanical properties due to GNP agglomeration [49].

GNP/Al composite of 0.1, 0.3, 0.5 wt% GNP were prepared by powder metallurgy and the various sintering time effect and sintering temperatures for density and hardness were studied. From the analysis, it is seen that 0.1wt%Gr provided good hardness having the best sintering time to be 180min and sintering temperature to be 630°C. Compared to pure Al, the hardness increased from 38HV to 57HV [50].

### 2.1.2 Importance of Aluminum –Carbon Composite

Carbon material has showed itself as a promising reinforcement for Aluminum matrix. Many form of carbon reinforcement such as Graphite, diamond, carbon fiber (3D), Graphene (2D) and CNT (1D) are used in different applications. But the main areas are aerospace, automobile and thermal management due to its low density, superior mechanical properties, thermal conductivity and low thermal expansion coefficient. It is very difficult to fabricate due to interfacial reaction, non-uniform properties and low wettability [24].

*Table 2: Carbon Aluminum composite and their processing route*

	According to Morphology	Continuous reinforcement	Carbon fibers and Carbon Foams
		Discontinuous reinforcement	Graphite, Diamond, CNTs and Graphene
		Laminate reinforcement	Carbon fibers

Carbon Aluminum composite	According to the processing technique	Liquid metallurgy processing	Stir casting	Carbon fibers /Al composite
			Gas pressure Infiltration	Carbon fibers, Graphite, Diamond/ Al composite
			Squeeze casting	Carbon fibers, Graphite/Al composite
			Ultrasonic Infiltration	Carbon fiber/Al composite
		Powder Metallurgy	Spark plasma sintering	Carbon fiber, diamond, CNT / Al composite
			Vacuum Hot pressing	Diamond, graphite, carbon fiber/Al composite

Flake powder metallurgy used to fabricate the carbon nano tube reinforced aluminum matrix composites were cold rolled to decrease the grain size. It was analyzed (fig. 5(a and c)) with the help of tensile tests at high temperature from 325 to 450 °C and strain rate was kept from  $4.17 \times 10^{-2}$  to  $2.09 \times 10^{-1} \text{ s}^{-1}$  to discover the grain refinement effect on the superplastic deformation behavior. After cold rolling, it was seen that the grain size was reduced averaging from 580nm to 300nm with improved uniformity. Whereas, at 400°C and  $4.17 \times 10^{-1} \text{ s}^{-1}$ , elongation to failure was enhanced by 40% related to that without being cold rolled. As seen in fig. 4(b and d), both uniform elongation and great elongation to failure was obtained as appropriate deformation conditions for the refined microstructure for 375 °C and intermediate strain rate [51].

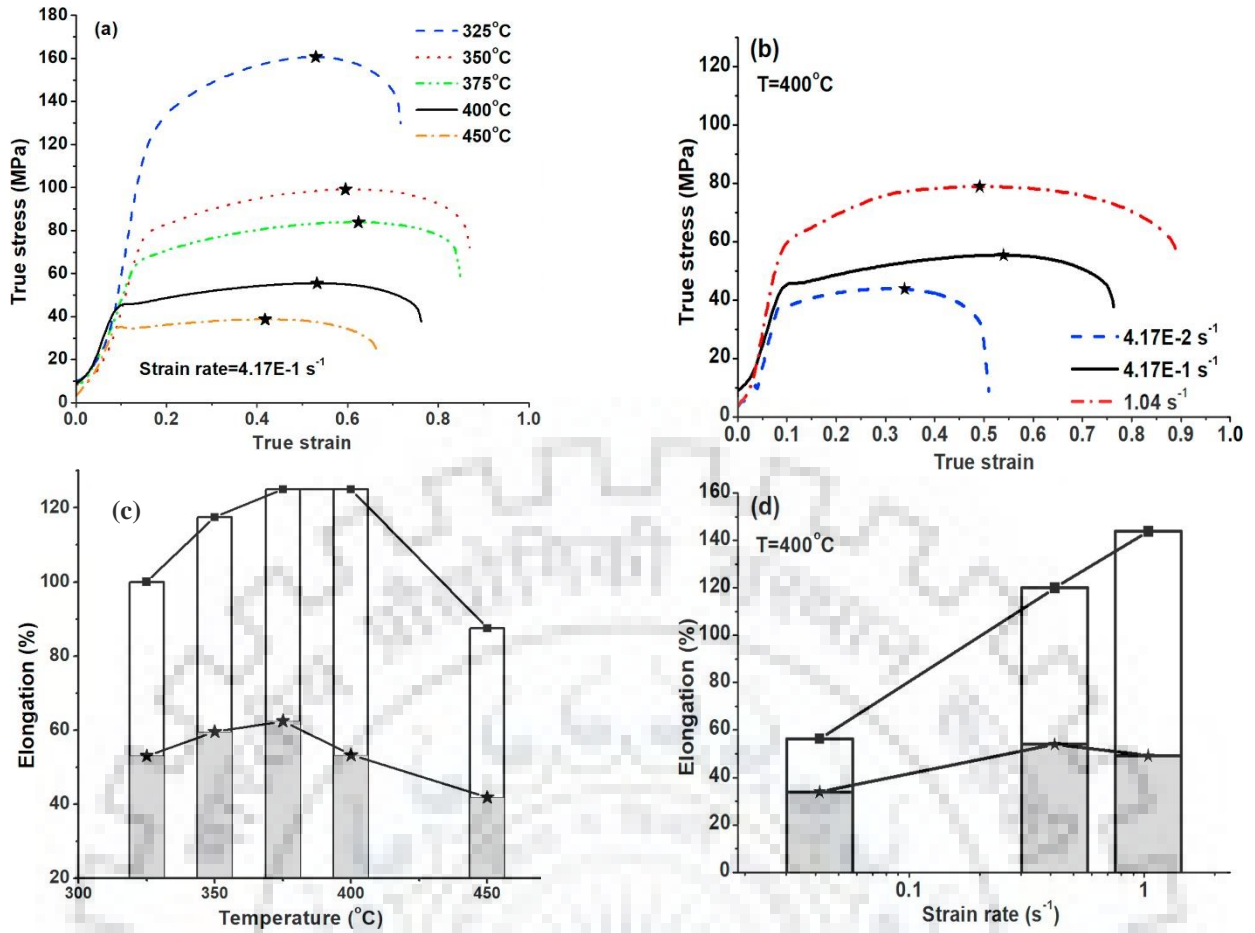


Fig. 6 Graph of true stress-strain for the cold-rolled samples under (a) Tensile testing at different temperatures with the same strain rate, (b) at 400°C, (c)(d) Plot of elongation to failure vs temperature (white column) and corresponding strain at which the maximum stress is reached (gray column)[51]

Another paper showed the results indicating that the tensile stress of the Al alloy decrease from 325 to

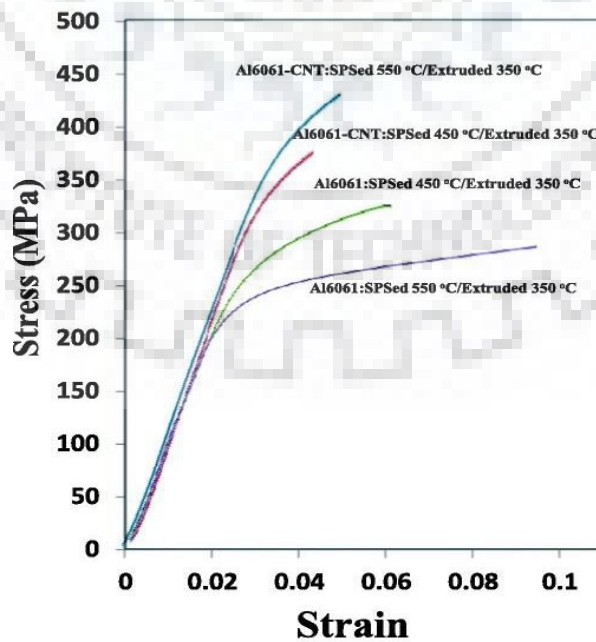


Fig. 5 Stress vs strain curve [52]

290 MPa with increasing sintering temperature from 450 to 550 °C, due to rapid grain growth of aluminum nanocrystals. On the contrary, the tensile strength of the nano-crystalline aluminum-CNT increased from 375 to 430 MPa with an increase in sintering temperature (fig. 6). Improved properties of Al6061/CNT nanocomposite is due to the homogenous distribution of CNT as reinforcement and its effect on the grain size stability even at higher sintering temperature [52].

A combination of ball milling and hot extrusion were used to prepare 0.5wt% GO reinforced Al matrix composite and 0.5wt% CNT reinforced Al matrix. The mechanical properties, microstructures and textures were compared with the pure Al as well as the interfacial reactions and the reinforcement structure were examined. It was observed that both the reinforcement was heterogeneously dispersed in the matrix, causing in the formation of agglomeration at the grain boundaries. It showed clustering was higher in CNT/Al compared to GO/Al composite. As a result, the GO/Al displays a more refined microstructure than pure Al that increased the mechanical properties due to the pinning effect shown by GO. On the contrary, the CNT/Al composite, with the mean grain size similar to the pure Al, shows reduced compressive yield stress (fig. 7), due to a low efficient load transfer causing from the huge agglomeration of CNT [53].

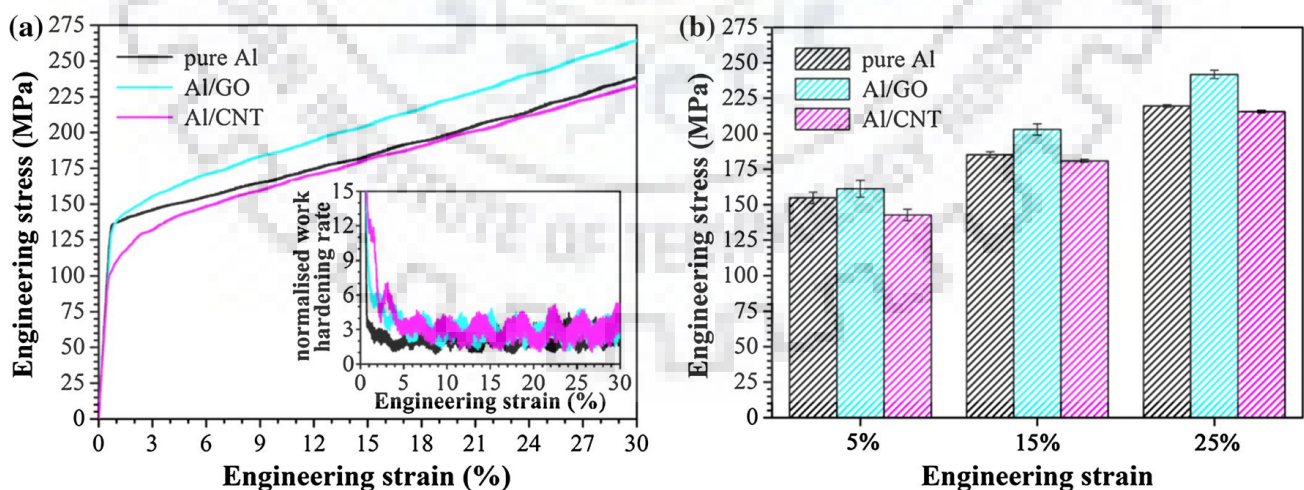


Fig. 7 Compression test for pure Al, GO/Al and CNT/Al composites. (a) Engineering stress–strain curves. The inset displays the corresponding normalized work hardening rate curves, (b) Average engineering stress at 5, 15 and 25% engineering strain [53]



## 2.2 IMPORTANCE OF SPARK PLASMA SINTERING

There are two ways to sinter carbon aluminum composite one is liquid metallurgy route and other one is powder metallurgy route. In liquid metallurgy route mixing of reinforcement in molten matrix of aluminum followed by solidification, the main drawback of liquid metallurgy processing is poor wettability of aluminum with graphene [8] because there is a huge difference between surface tension of aluminum (955mN/m, at its melting point) and graphene (79-155mN/m). That is why contact angle between aluminum and graphene is high, which causes reduce in mechanical properties. On the other hand Powder metallurgy is widely used for fabrication of most carbon aluminum composite.

In powder metallurgy route, interfacial reactions reduces due to consolidation at relatively low temperature. In powder metallurgy route also, there are different method to sinter but for consolidation of carbon aluminum composite two methods have been reported, vacuum hot pressing and spark plasma sintering. In vacuum hot pressing container is heated by radiation through external heating element thus powder is consolidated through indirect heating in which conduction occurs from container wall. Thus large amount of heat energy wasted in the environment. While in spark plasma sintering is electric current assisted /activated sintering process. In this process, powder consolidation done by the application of heat and pressure simultaneously due to flow of electric current. Joule heating as well as localized Spark formation between the gaps of powder decreases porosity gradually. Due to shorter sintering time grain coarsening and unwanted reaction can be easily turn away. Current and temperature distribution is a deciding factor for proper density distribution. In the beginning of current flow, large density variation prone to localized overheating and melting.

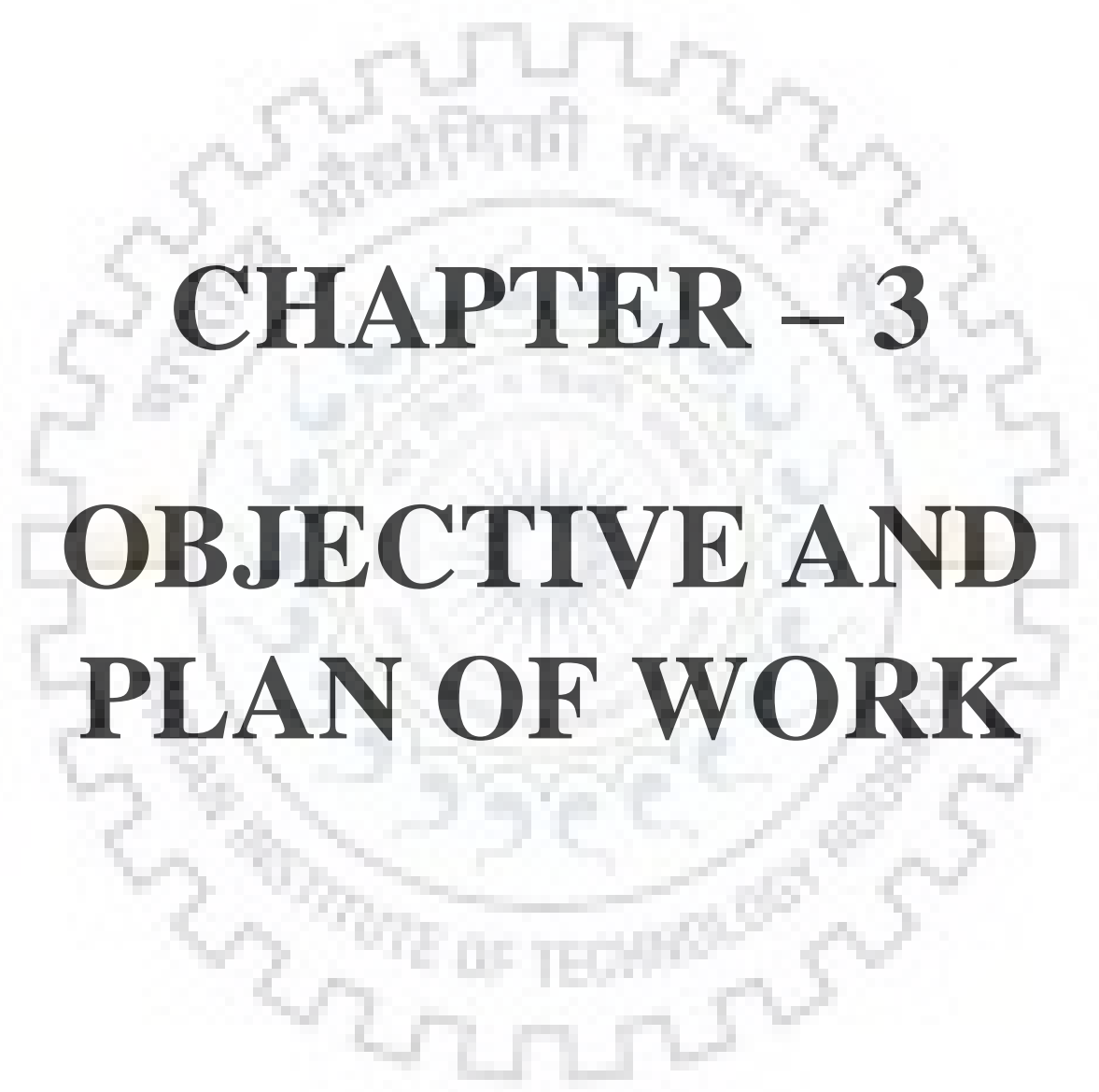
Table 3: Production methods and their advantage/ disadvantage

Approach	Methods	Procedure	Advantage/disadvantage
Top-down approach	Micromechanical cleavage	Scotch tape method which produce Graphene by repeated cleavage	High quality Graphene produced but slow method
	Electrochemical exfoliation	Graphite is exfoliated into Graphene by electrochemical reaction. Graphite electrode decomposes and Graphene is collected from electrolyte	Electrolytic surfactants molecule are difficult to remove which affects electrical properties
	Solvent-based exfoliation	Thermal exfoliation of Graphite to form GICs Exfoliation of Graphite in solvent by sonication method Hummers Method	surfactants molecule are difficult to remove
	Unzipping carbon nanotubes	Wet chemistry and physical methods	These nanoribbons have different than pristine graphene
Bottom-up approach	Epitaxial growth	Deposition of Graphene on the surface of SiC at high temperature and vacuum by graphitization of carbon atom on SiC surface	Highly expensive and bi-layer and Mono-layer Graphene is difficult to produce
	Chemical vapor deposition (CVD)	Pyrolysis of methane on metal substrates. Optimum condition	Number of layers are totally depend on process

		totally depends on metal substrates surface	parameters, monolayer Graphene can be produced
--	--	---------------------------------------------	------------------------------------------------

Graphene and CNT based aluminum matrix composite upto 1wt% reinforcing content were fabricated through SPS, microwave and conventional method at 450, 600 and 700°C temperature, respectively.  $Al_4C_3$  was observed in other two techniques except for SPS process. Moreover, SPS offered uniform distribution of CNT and GNP reinforcement compared to other method [54]. Till date, no literature is available for thermo-mechanical treatment of GNP/Al composite and its effect on the final properties of the structure.





**CHAPTER – 3**

**OBJECTIVE AND  
PLAN OF WORK**

### 3. OBJECTIVES AND PLAN OF WORK

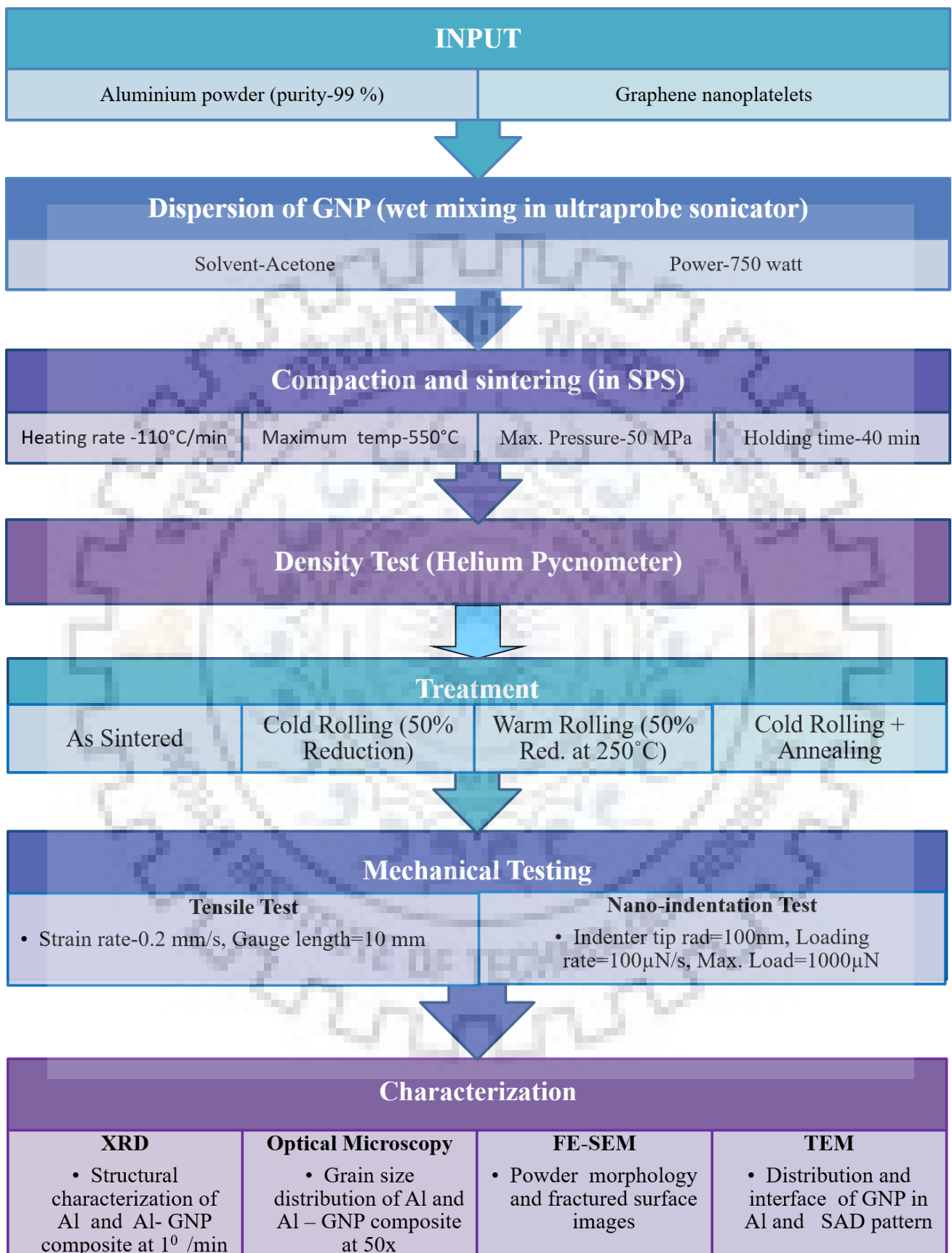
#### 3.1 OBJECTIVES OF WORK

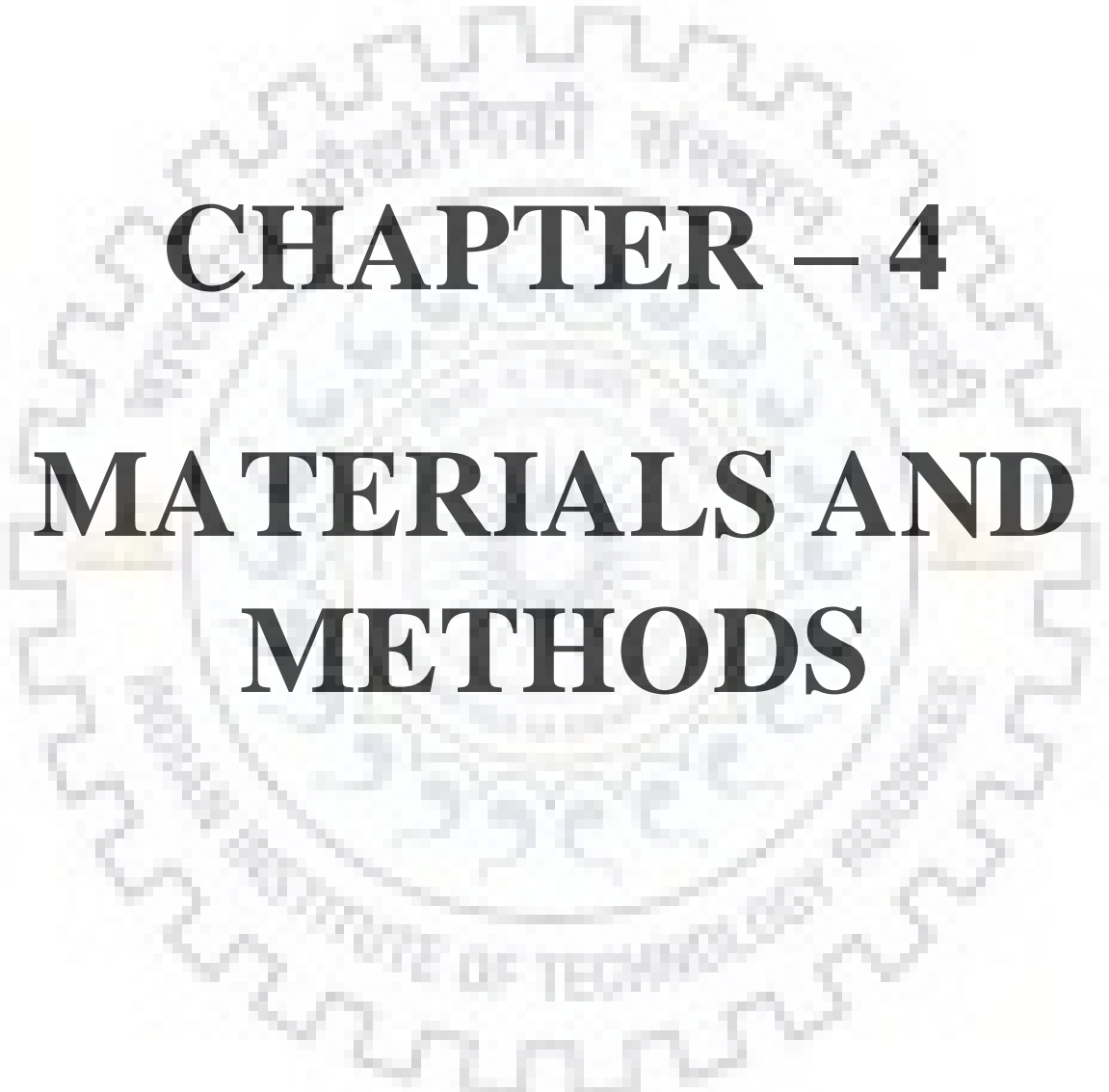
From the literature survey it is seen that agglomeration takes place above 1 wt% reinforcement content, so thermo-mechanical treatment is implemented to further enhance the mechanical properties of GNP/Al composite.

The specific aim of the study is:

- 1) To observe the mechanical behavior of GNP in Al matrix, fabricated by spark plasma sintering (SPS)
- 2) Carrying out of post treatment process, like, rolling at room temperature, warm rolling and rolling followed by annealing.
- 3) Identification of  $Al_4C_3$  formation by XRD and TEM.
- 4) The composite is assessed for ultimate tensile strength, yield strength, toughness, % strain (upto fracture), elastic modulus and hardness at different steps (i.e. sintered, cold rolled, warm rolled and rolled + annealed).

### 3.2 METHODOLOGY





**CHAPTER – 4**  
**MATERIALS AND**  
**METHODS**

## 4. MATERIALS AND METHODS

GNPs were purchased from XG-Sciences (Lansing, MI, US) of Grade M having the density of 2.2 g/cm<sup>3</sup> and surface area of 120-150 m<sup>2</sup>/g [55]. They consist of irregular shaped flakes with mean particle

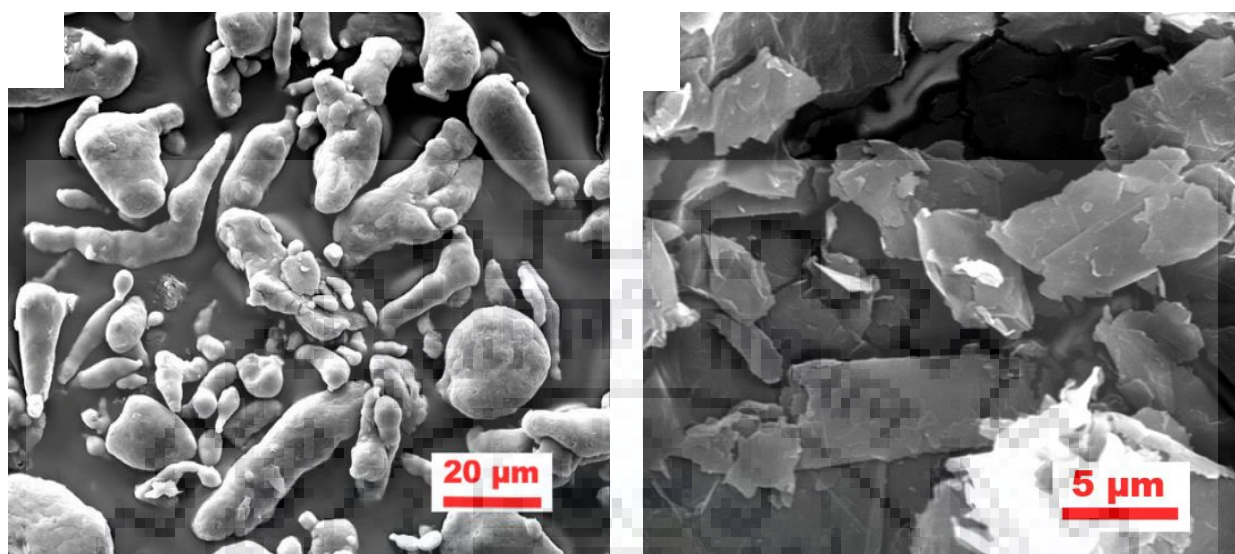


Fig. 8 SEM images of (a) Al, (b) GNP

size of 5-7 μm and thickness of 6-8 nm. Aluminum powder were acquired from Sisco Research Laboratories Pvt. Ltd. (Maharashtra, India) having 99% purity and ~325 mesh. It comprises of 0.1% Fe, 0.1% Si, 0.02% Cu, 0.02% Mn and 0.03% Ti. Fig. 8(a and b) indicates the SEM micrographs of powdered samples for Al and GNP.

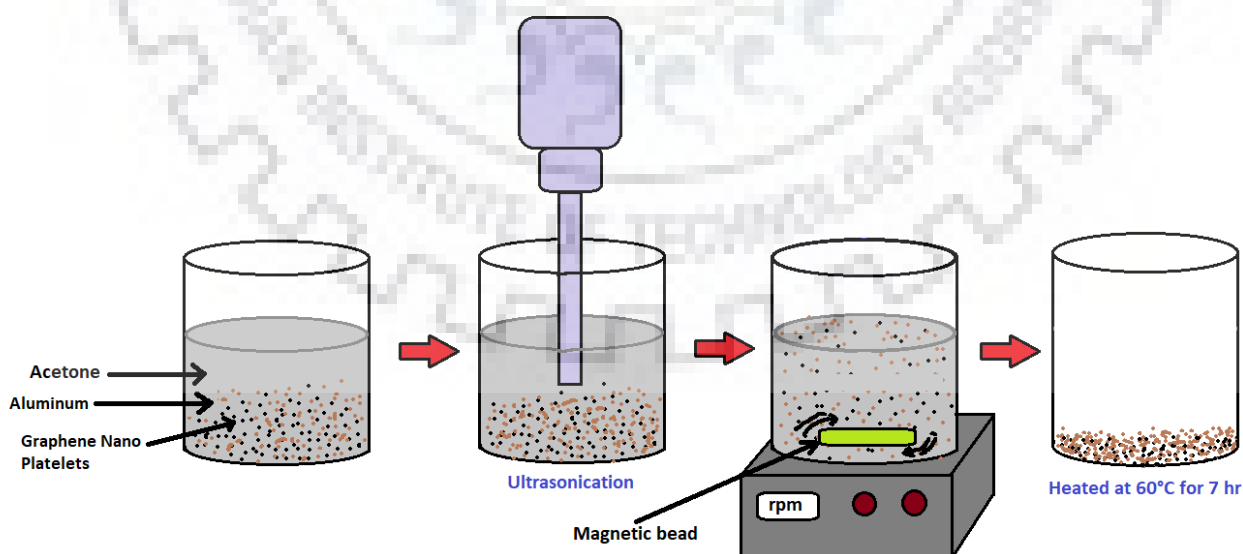


Fig. 9 Process for mixing the Al and GNP powder



## 4.1 FABRICATION OF COMPOSITES

Powders with reinforcement content 0, 0.5, 0.75 and 1wt% were prepared by means of ultra-sonication

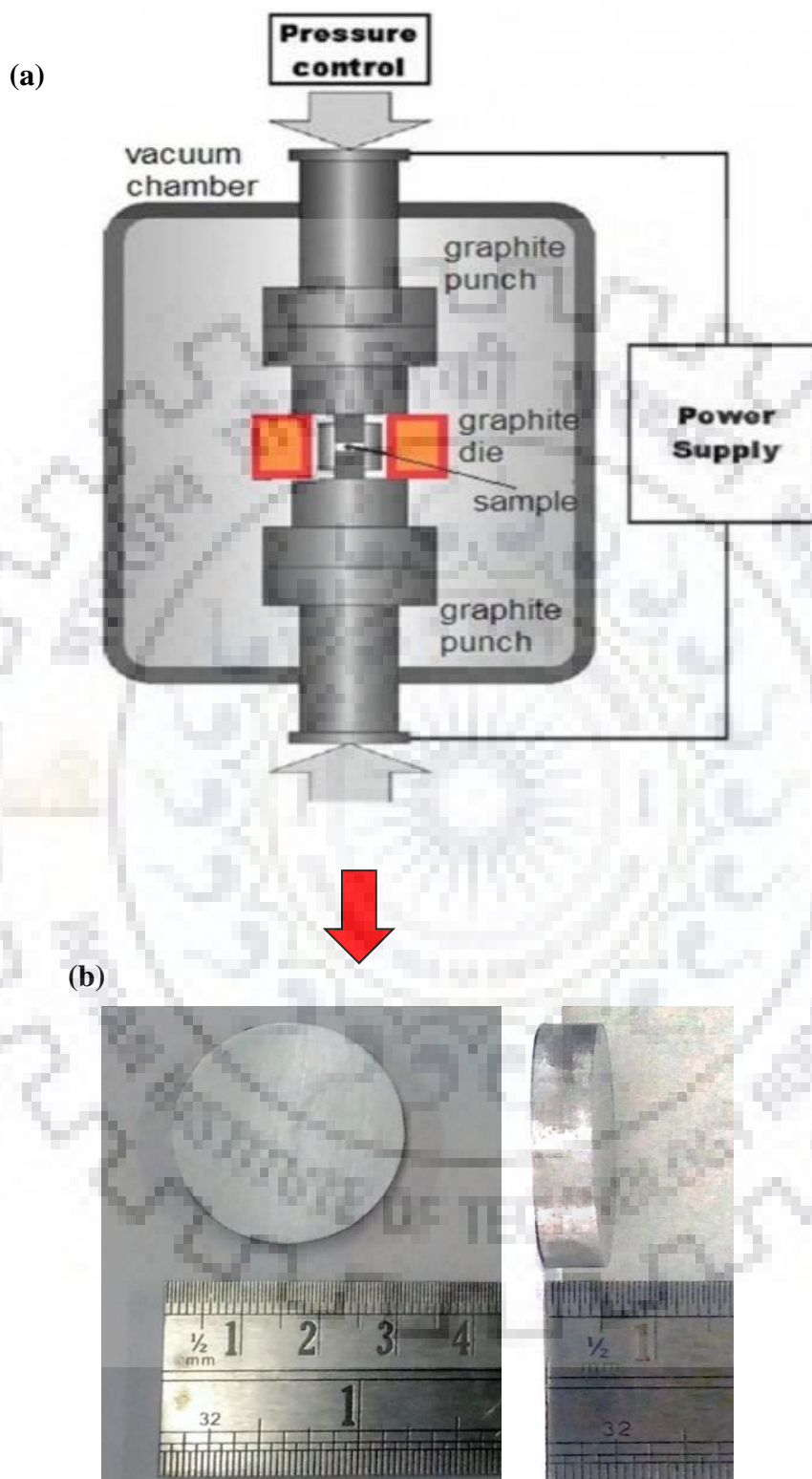


Fig. 10 (a) Layout of the SPS inner chamber and (b) Prepared sample from SPS

process, acetone was used as a solvent to disperse GNPs. Probe-sonicator (PKS – 750F, PCI Analytics

Pvt. Ltd., Mumbai, India) was used for ultra-sonication for 40 min with 5 sec sonication and 3 sec gap. Meanwhile, the Al powder was added in parts for every 5 min within 30 min. The solution was mixed using magnetic stirrer till the solvent dried up and further kept in hot air oven at 60°C for 7 hr to remove any moisture remnant (fig. 9). It was then sintered by Spark Plasma Sintering (SPS) method (fig. 10(a)) (Dr. Sinter, SPS- 625 Japan) in inert argon atmosphere with the maximum temperature and pressure set at 550°C and 50 MPa, respectively, having a holding time of 40 min. Pellets of 5 mm thickness and 30 mm diameter were prepared as seen in fig. 10(b). The advantage of using SPS process is to obtain high-densified material for less holding time compared to the conventional sintering process [45]. Joule heating as well as localized Spark formation between the gaps of powder decreases porosity gradually. Due to shorter sintering time grain coarsening and unwanted reaction can be easily turn away. The pellets were then cut into section of 30mm x 5mm for post-treatment such as: (i) Cold rolling at room temperature, (ii) Warm rolling at 250°C and (iii) Rolling followed by annealing at 250°C. Each sample was rolled with thickness reduction of 50% in 3 passes. For Room temperature rolled, warm rolled and room temperature rolled + annealed RR, WR and RA will be used in the terminology, respectively.

## 4.2 MECHANICAL AND STRUCTURAL ANALYSIS

The experimental densities of as-sintered composites were calculated using helium pycnometry, (Smart pycno 32, Mumbai, India). In order to identify any unwanted phase produced during sintering process, the composites were characterized using X- Ray Diffractometer (Smart lab, Rigaku Japan) with Co K $\alpha$  radiation for a 0.02° step size, scan rate of 1°/min and 2 $\theta$  range of 5–90°. Grain sizes of as-sintered and rolled samples for various conditions were estimated under optical microscopy captured by Leica DM2500 (Leica Microsystems Inc., USA). For microstructural characterization, the samples were made by emery paper from 320 to 2000 grit size and cloth polished with the help of 1

$\mu\text{m}$  alumina, and then etched using Keller's reagent (95 mL water, 1.5 mL HCl, 2.5 mL HNO<sub>3</sub> and 1.0 mL HF)



*Fig. 11 Section cut for tensile test*

The samples were cut into dog-bone shaped specimen as per B557 ASTM standard for studying tensile properties by using universal testing machine (Hounsfield, model ZD-20, USA) at a strain rate of

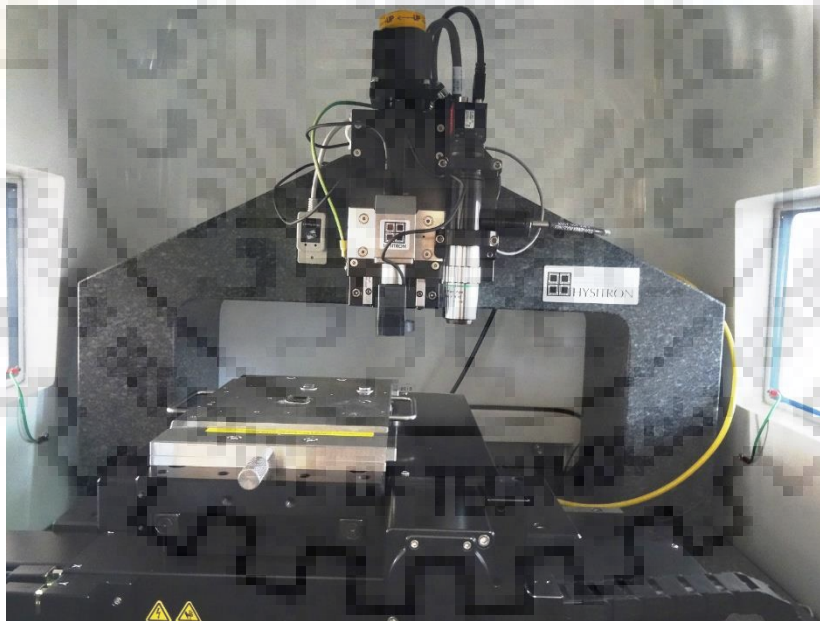


*Fig. 12 Hysitron TI-950 Triboindenter*

0.2mm/s. It was cut with cross-section of  $3.8 \times 1.6 \text{ mm}^2$  and gauge length of 10 mm (fig. 11). The samples for the rolled pellets were cut along rolling direction. Powder morphology and fractographic analysis was done using energy dispersive spectroscopy (EDAX-Metek, USA) and scanning electron

microscope (FEI Quanta 200F, Switzerland) with an accelerating voltage of 20 kV. Transmission electron microscope (TEM) (JEM 3200FS, USA) was used to determine the embedment of GNP in the matrix and dislocation behavior. The samples were prepared by mechanical polishing and ion thinning with the help of Gatan Precision Ion Polishing System II at 5 kV. Hardness and elastic modulus were determined by nano-indentation test using Hysitron TI-950 Triboindenter (Hysitron Inc., USA) (fig. 12), with tip radius of 100 nm having loading rate of 100  $\mu\text{N/s}$  with maximum load of 1000  $\mu\text{N}$ . For each sample, minimum 25 indents were done to obtain average elastic modulus and hardness.





# **CHAPTER – 5**

# **RESULTS AND DISCUSSION**

## 5. RESULTS AND DISCUSSIONS

### 5.1 MORPHOLOGY OF GNP/AL COMPOSITES

Dispersion of GNPs in Al is shown in fig. 13 The effect of GNP dispersion in Al matrix is revealed in the optical images, which has influenced the shape and size of the grains. Pure Al as-sintered (Fig. 14(a)), indicates the bimodal structure of both large and small grains[56]. As seen from fig. 14(b and c) as the GNP content increases from 0.5 and 0.75 GNP/Al, respectively, it starts to agglomerate along the grain boundary which can be evidenced as a black region causing a non-uniform distribution of reinforcement. In addition to this, increasing the particle size of the GNPs increases the porosity, however sintering temperature reduces the defect caused by porosity [5][57]. The particles adjacent to

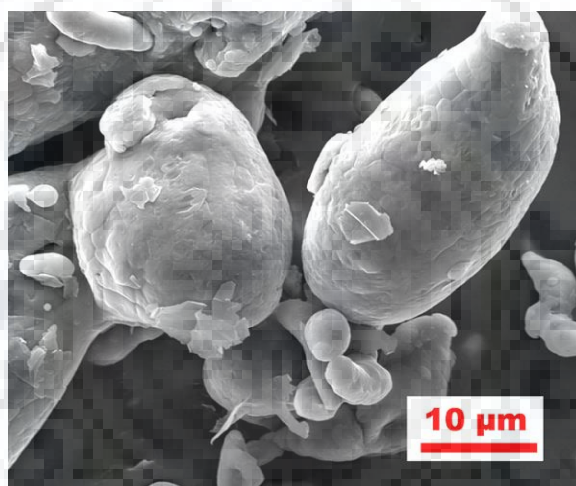


*Fig.13 SEM image of 0.75GNP/Al powder*

agglomerated GNP are comparatively small than those away from it, as the agglomerated GNP hinder grain growth by grain boundary pinning. The same can be evidenced from table 5 which contains the average grain size measured for all compositions at different conditions. Rolling has relatively substantial effect on the grain size, shape and orientation. Fig. 14(d-f) clearly shows that the grains tend to elongate and align along the rolling direction. During the warm rolling, the aluminum becomes more ductile and deform which gives way to dislocation to move on loading and simultaneously shears GNP along the grain boundary. This results in the further thinning by delamination of GNP, breaking the weak secondary force, dispersing the agglomeration (fig. 14 (d-l)) and forming a nice and smooth



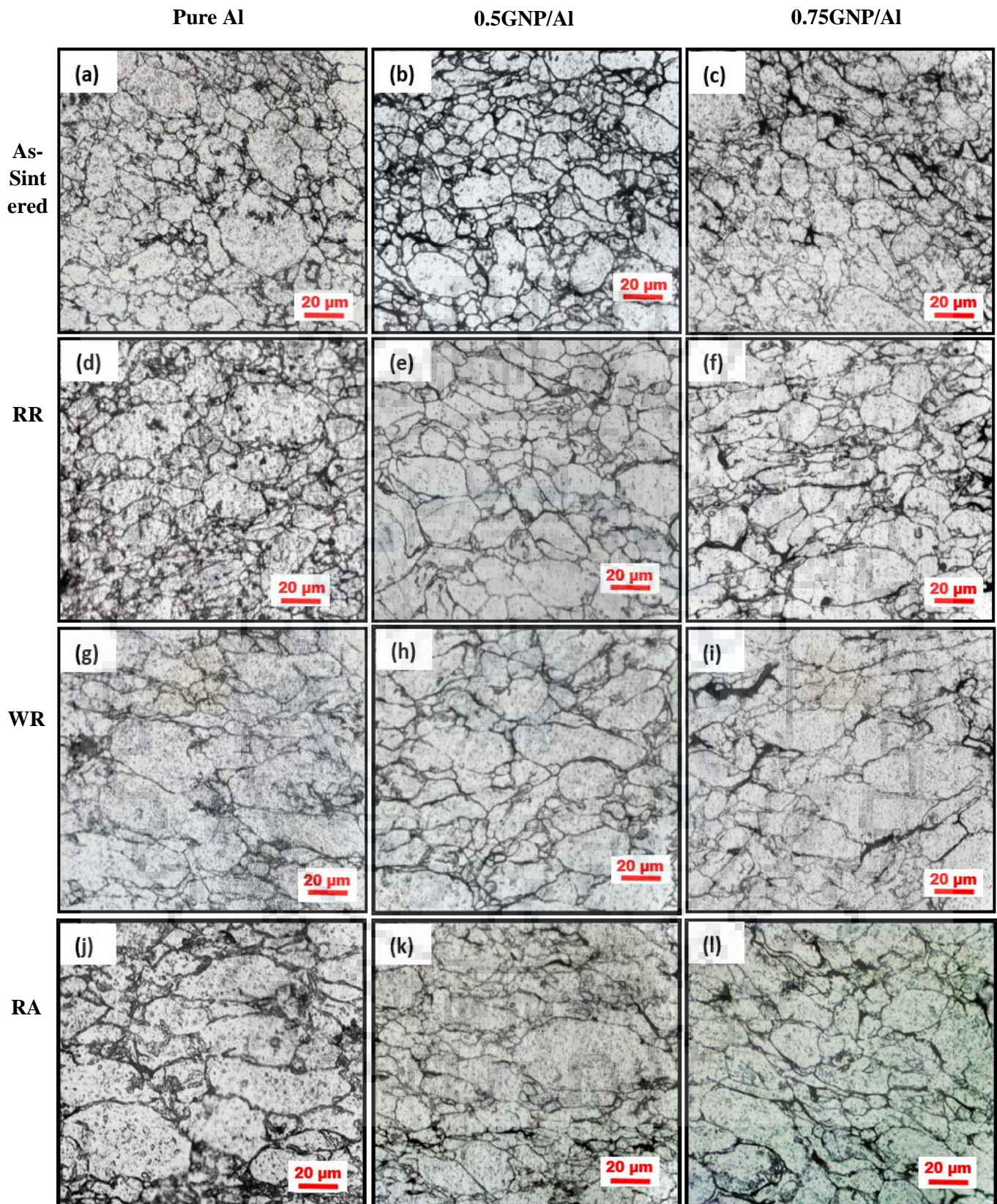


Fig. 14 Optical microscopy of (a)(d)(g)(j) Pure Al, (b)(e)(h)(k) 0.5GNP/Al and (c)(f)(i)(l) 0.75GNP/Al for As-Sintered, RR, WR and RA condition, respectively.

interstitial bonding at the boundary. During WR and RA, the difference in the optical microstructure

indicates the verge in the activation of recrystallization process as few sub grain formation is observed.

The distribution of GNP through EDS mapping is shown in fig. 15(a and b).

*Table 4*  
*Average grain size( $\mu\text{m}$ ) of composites at different conditions*

Composite	As-Sintered	RR	WR	RA
Pure Al	25.36	28.14	39.74	37.68
0.5GNP/Al	22.04	25.28	35.17	32.24
0.75GNP/Al	17.11	22.65	30.43	27.67

Deformation rate  $\varepsilon$  for rolled samples were calculated using Ekelund formula [58][34]:

$$\varepsilon = \frac{2v \sqrt{\frac{h_0 - h_1}{R}}}{h_0 + h_1} \text{----- (1)}$$

Where, R is the radius of the roller drum with 55 mm;  $v$  is the rolling speed with 21.6 mm/s;  $h_0$  and  $h_1$  are the thickness of the sample before and after rolling.

*Table 5*  
*Parameters for rolling process*

Pass	Reduction (mm)	$h_0$ (mm)	$h_1$ (mm)	$\varepsilon$ (s <sup>-1</sup> )
1	0.58	3.5	2.92	0.7
2	0.92	2.92	2.30	0.9
3	0.38	2.30	1.75	1.1

The fracture surface of the pure Al as-sintered displayed in fig. 16(a) show spherical dimples, which is a characteristic of transgranular ductile fracture mode, while fig. 16(b and c) shows micro-void coalescence due to GNP particles. The presence of GNP is shown by dotted circles. The dimples are visible less in higher GNP loading where intergranular fracture is emerging indicating the brittleness.



For instance in fig. 16, the surface near the presence of GNP (shown by thick arrows) was ripped off. This intergranular fracture of grain boundary is due to the dislocation piling up by the GNP.

Throughout the fracture surface of 0.5 and 0.75GNP/Al WR presented in fig. 16(g-i), deep dimples appear in adequate quantities, which shows mainly transgranular ductile fracture mode (also having

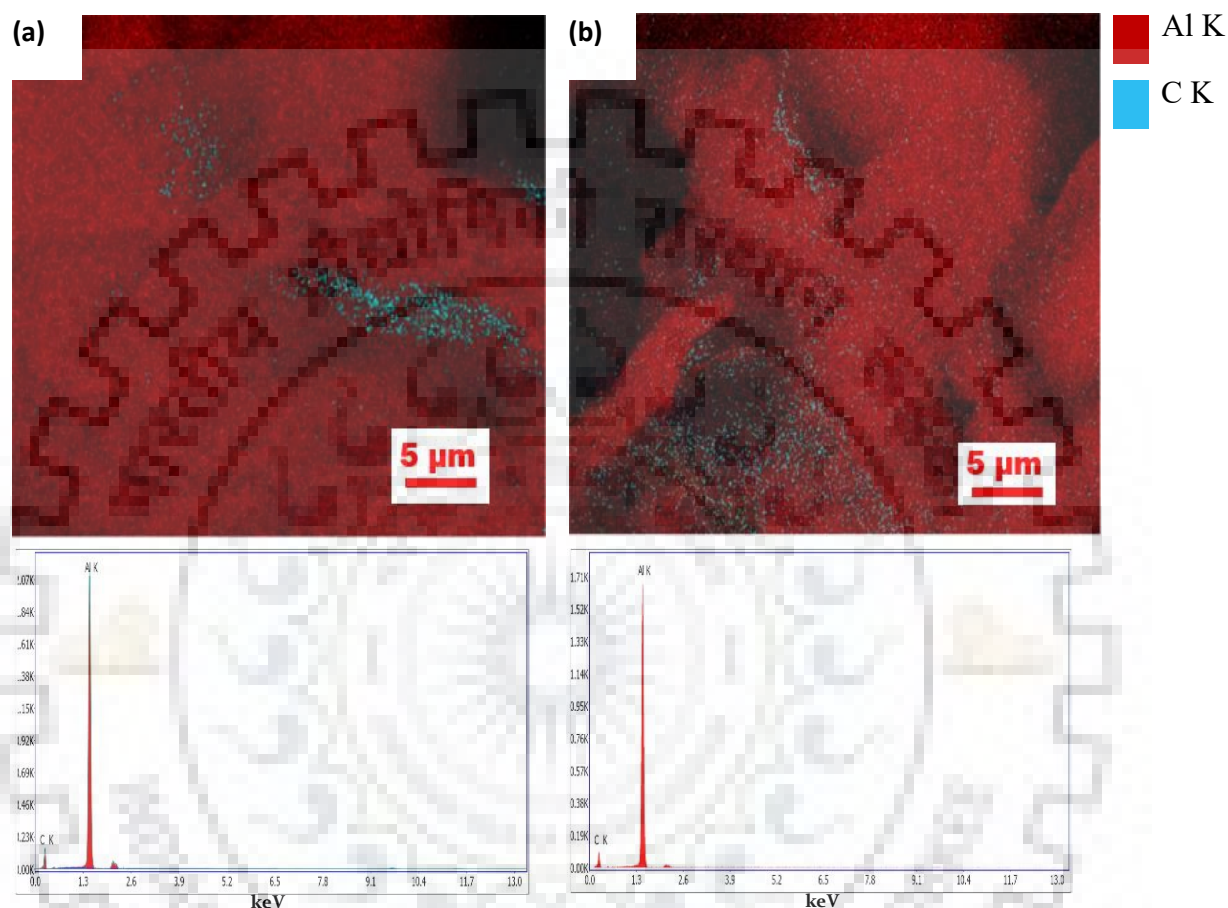


Fig. 14 EDS mapping of (a) 0.5GNP/Al and (b) 0.75GNP/Al

supplementary intergranular fracture), compared to 0.5 and 0.75GNP/Al RR (fig. 16(d-f)), with less plastic deformation concentrated at grain boundaries while the uneven fracture indicates that the crack propagation path is altered several times during tensile investigation. This deep dimples and uneven surface showing sufficient ductile deformation is due to finer particles. The numerous micro-voids and cavities, as indicated, were noticed in all condition of 0.75GNP/Al indicating the degradation of the composite with further addition of reinforcement. The bonding energy at interface of 1wt% GNP/Al is reduced due to the large number of gaps and cracks in the agglomerated plates, which ultimately



deteriorated the mechanical properties of the composite leading to irregularities and rise in stress concentration (not discussed here). In addition, as GNP is a multi-layer graphene, the bonding force is much weak between the graphene inter layers. The agglomerated plates turns into graphite which is

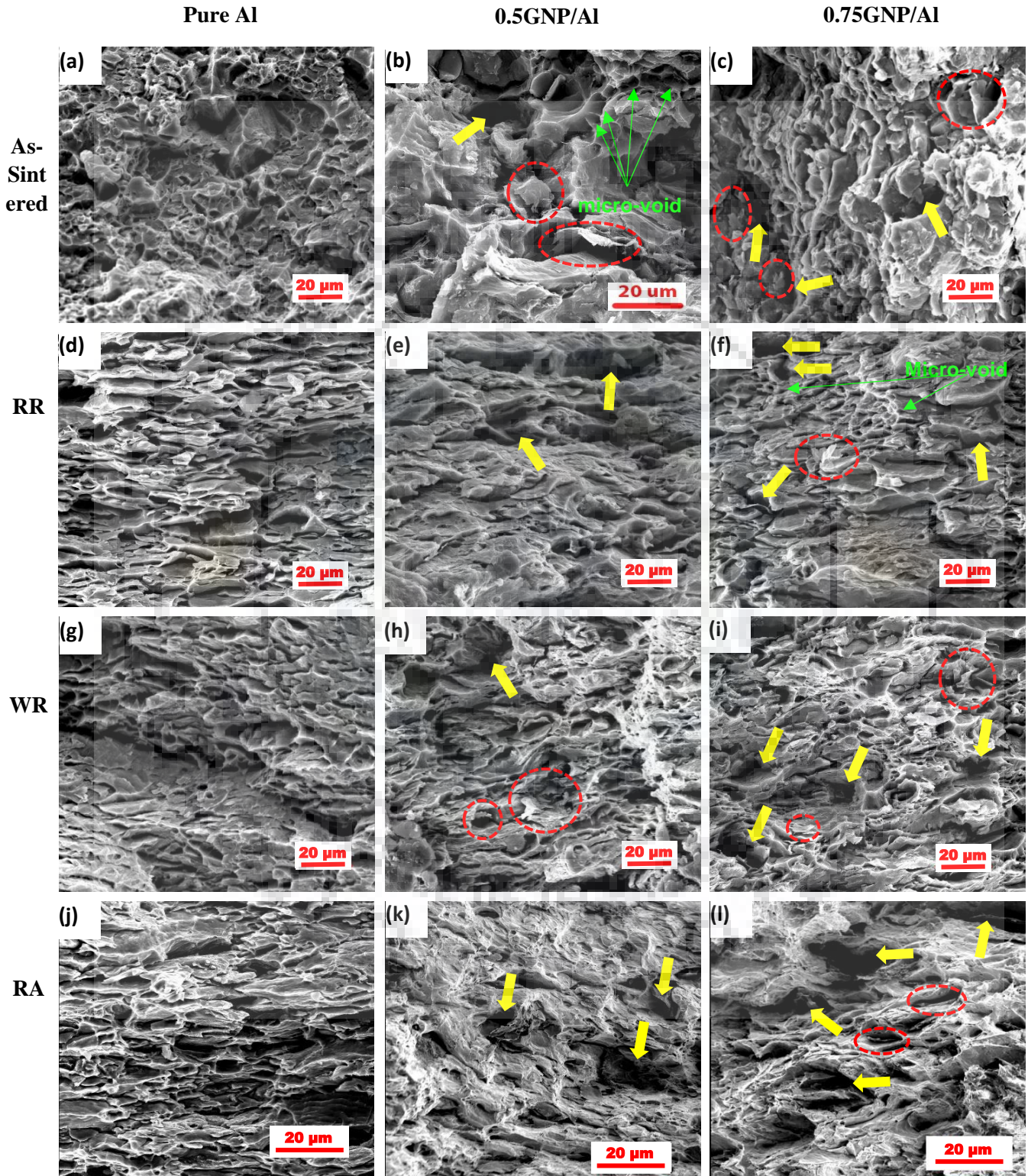


Fig. 15 SEM micrographs of (a)(d)(g)(j) Pure Al, (b)(e)(h)(k) 0.5GNP/Al and (c)(f)(i)(l) 0.75GNP/Al for As-Sintered, RR, WR and RA condition, respectively. Voids are indicated by arrows while GNP with dotted circles



the reason for its deterioration[43]. The samples which were rolled and annealed at 250°C shown in fig. 16(j-l) were having tearing morphologies indicating a quasi-cleavage fracture phenomena[59].

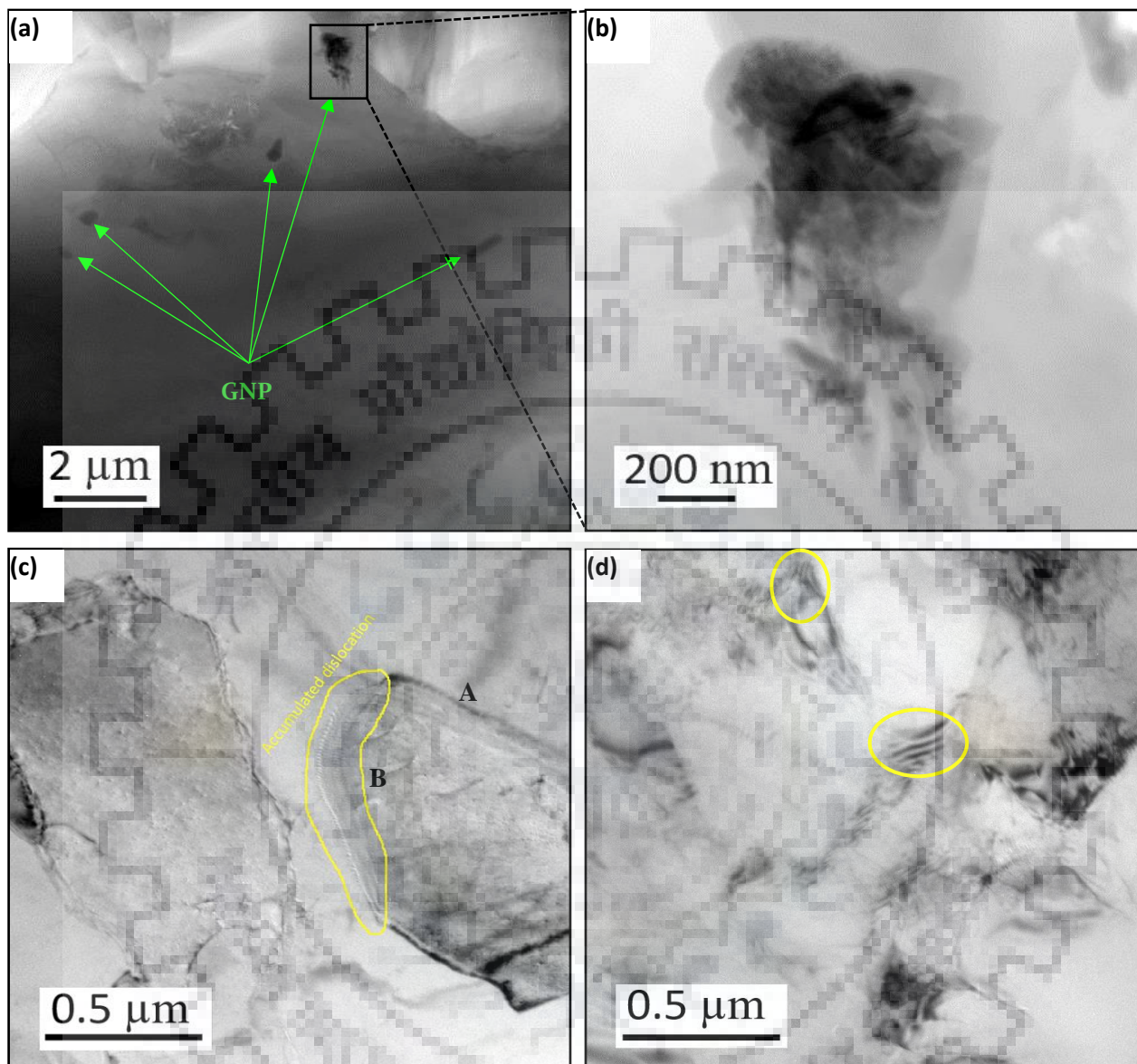


Fig. 16 TEM images of 0.5GNP/Al (a), (b) As-sintered and (c), (d) RR

The TEM images (fig. 17) also reveal the distribution of GNP along with the accumulated dislocation and highly deformed region along the matrix boundary (fig. 17(c and d)). The GNP particles embedded on the matrix surface and the sub-layers of graphene is seen in fig. 17(a and b). The dislocations accumulated at the grain boundary region results in the formation of the grain boundary lines shown by A and B in fig. 17(c). Rolling reduction accelerates both stored energy and precipitation giving rise to prominent dislocation entanglement. During plastic deformation, particles affect the dislocation

density, inhomogeneity of deformation in the matrix and deformation structure. Consequently, the recrystallization behavior is also affected due to the influence of reinforcement particles by driving force and nucleation sites for recrystallization in the vicinity. If the applied stress is resisted by the particle, then the dislocation proceeds to surround the particle and generates an Orowan loop at the particle-matrix interface, or else it deforms [60].

## 5.2 STRUCTURAL CHARACTERIZATION OF GNP POWDER AND GNP/AL COMPOSITE

The peaks of GNP (fig. 18) for 0.5 and 0.75GNP/Al in the XRD patterns are not visible as seen for pure GNP peak of (002) at  $30.7^\circ$  as it is below the detection limit ( $<1\%$  volume)[61]. The formation of  $Al_4C_3$ , which has a detrimental effect on the mechanical properties and shows a strong dependence on processing temperature, is also absent due to the sintering process by SPS that offers short time consolidation at low temperature. Nevertheless, the literature also states that a few amount of carbide formation results in good interfacial bonding[62]. Theoretical densities were estimated using rule of mixtures. Relative densities, compared to theoretical one, calculated for as-sintered samples showed

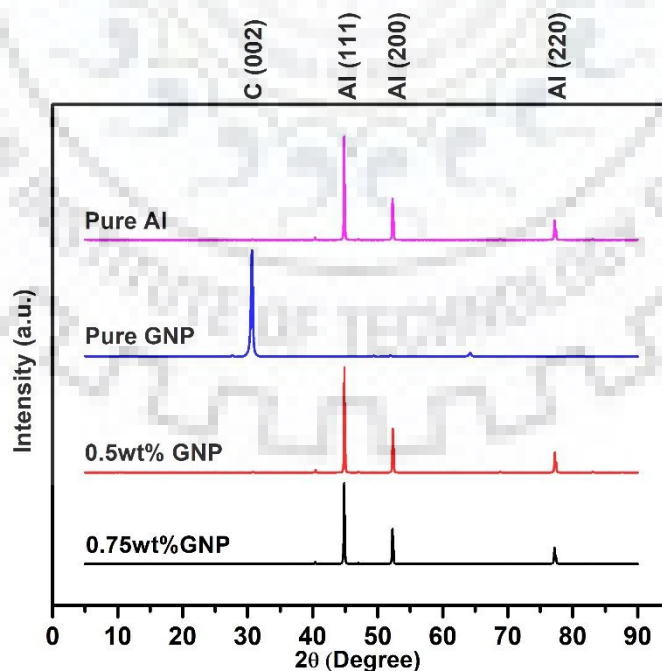


Fig.17 XRD graph for Pure Al, Pure GNP and GNP/Al

99.37%, 99.63% and 99.26% for pure Al, 0.5 GNP/Al and 0.75GNP/Al owing to proper reinforcement-

matrix bonding. However, further increase in GNP content affected the density due to pores and cavities observed in SEM images.

### 5.3 MECHANICAL BEHAVIOR OF COMPOSITES

The engineering stress-strain curves of the tensile tests of the GNP/Al as-sintered, RR, WR and RA are shown in fig. 19(a-d), respectively. The strength and ductility of the as-sintered composite with

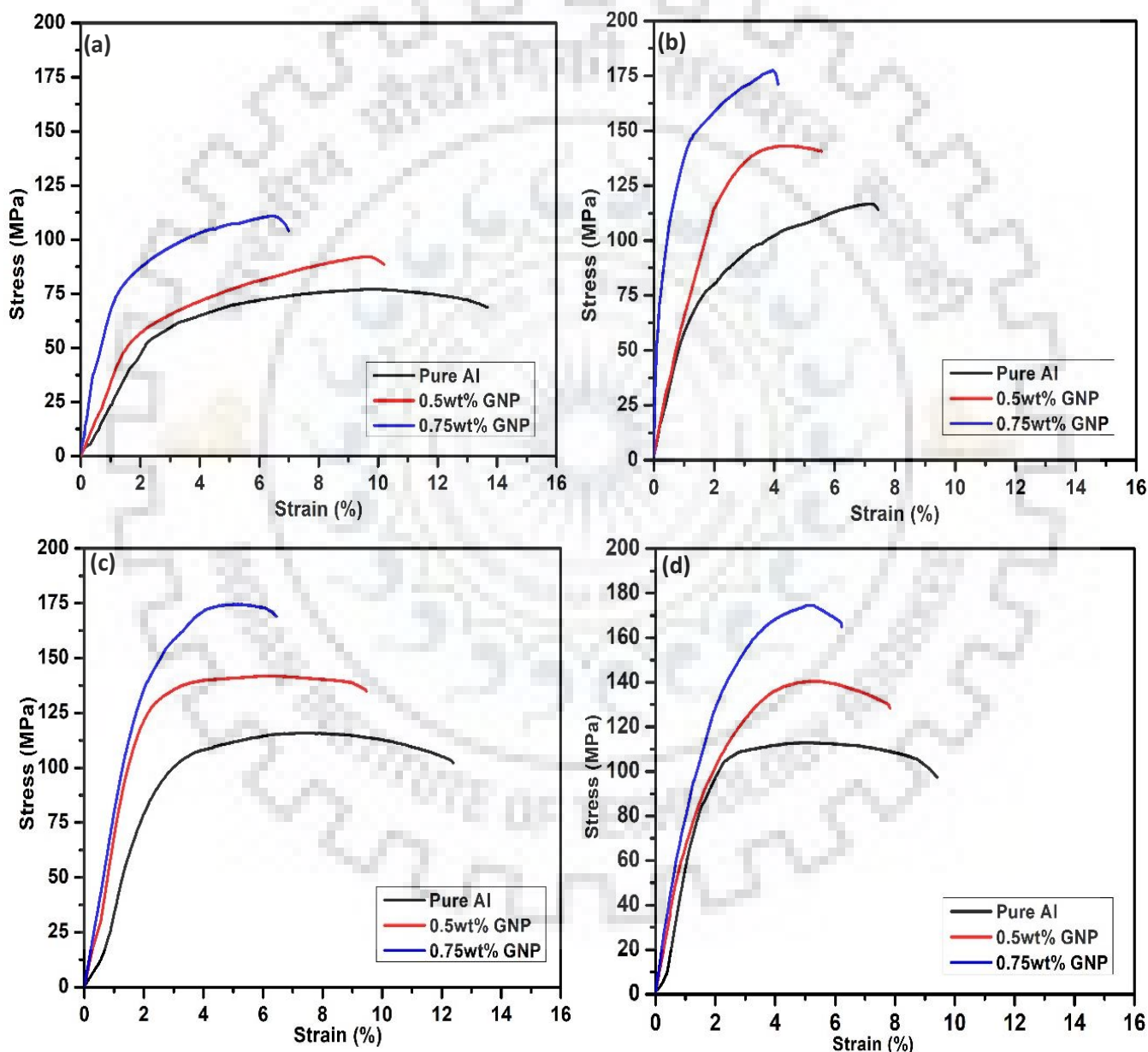


Fig.18 Tensile stress-strain curve of (a) As Sintered, (b) RR, (c) WR and (d) RA for different composites

0.75GNP/Al addition are 111 MPa and 7%, respectively, having strength enhancement by 44.1% and

ductility degradation by 49%, as compared to pure Al. GNP, having larger aspect ratio, assisted larger load transfer, providing efficient utilization of reinforcement. The increase in the dislocation density caused by rolling further strengthened the material. After the plastic deformation, grain refinement and small GNP particles substantially improved the strength as seen in fig. 20(a and b). The mismatch

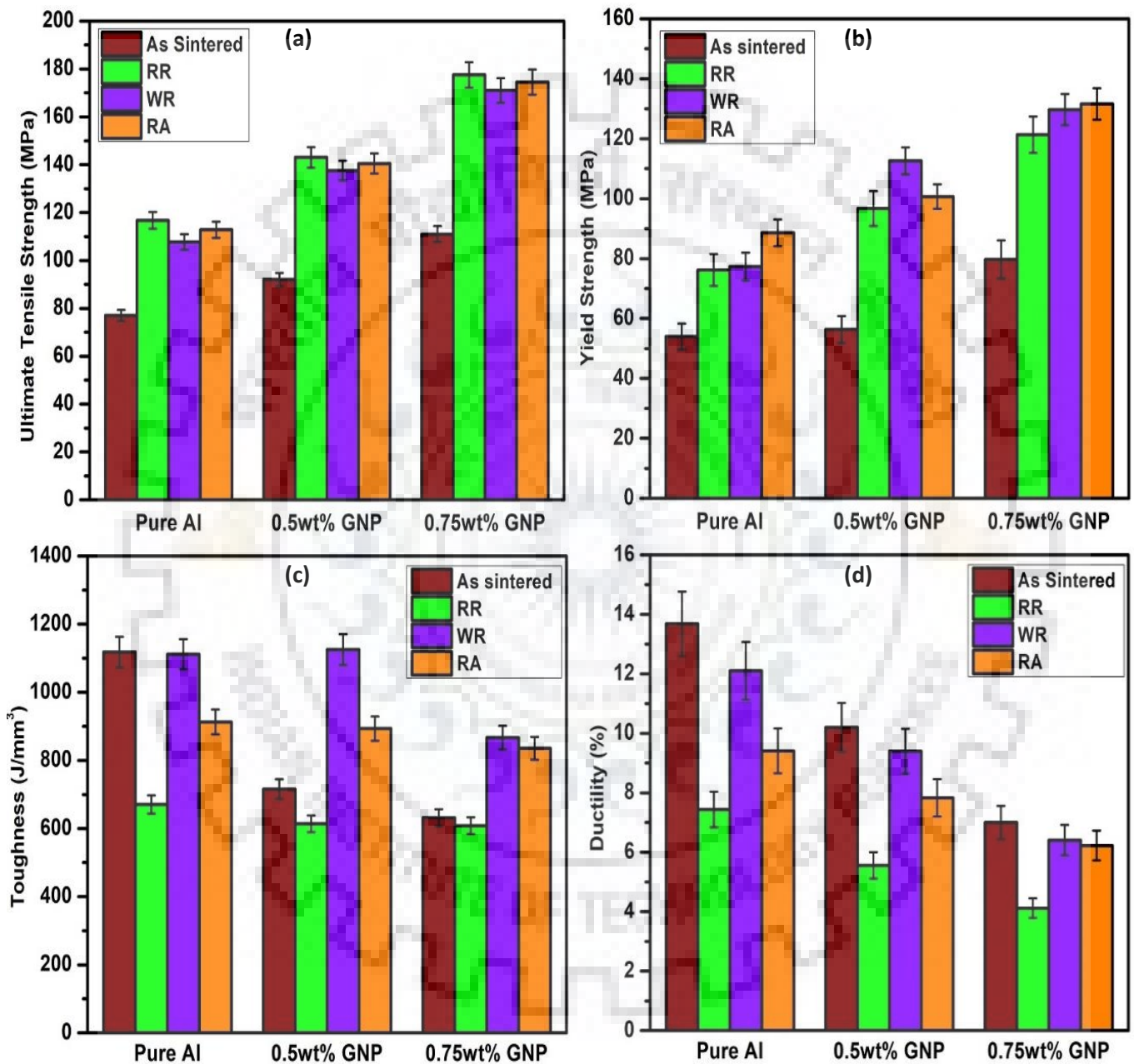


Fig. 20 Variation of (a) Ultimate Tensile Strength, (b) Yield Strength, (c) Toughness and (d) Ductility of different composites for as-sintered, RR, WR and RA conditions



between elastic modulus of GNP and Al resulting in the dislocation pile-ups increased the strain hardening of the composite during plastic deformation. While warm rolling, there is an increment in

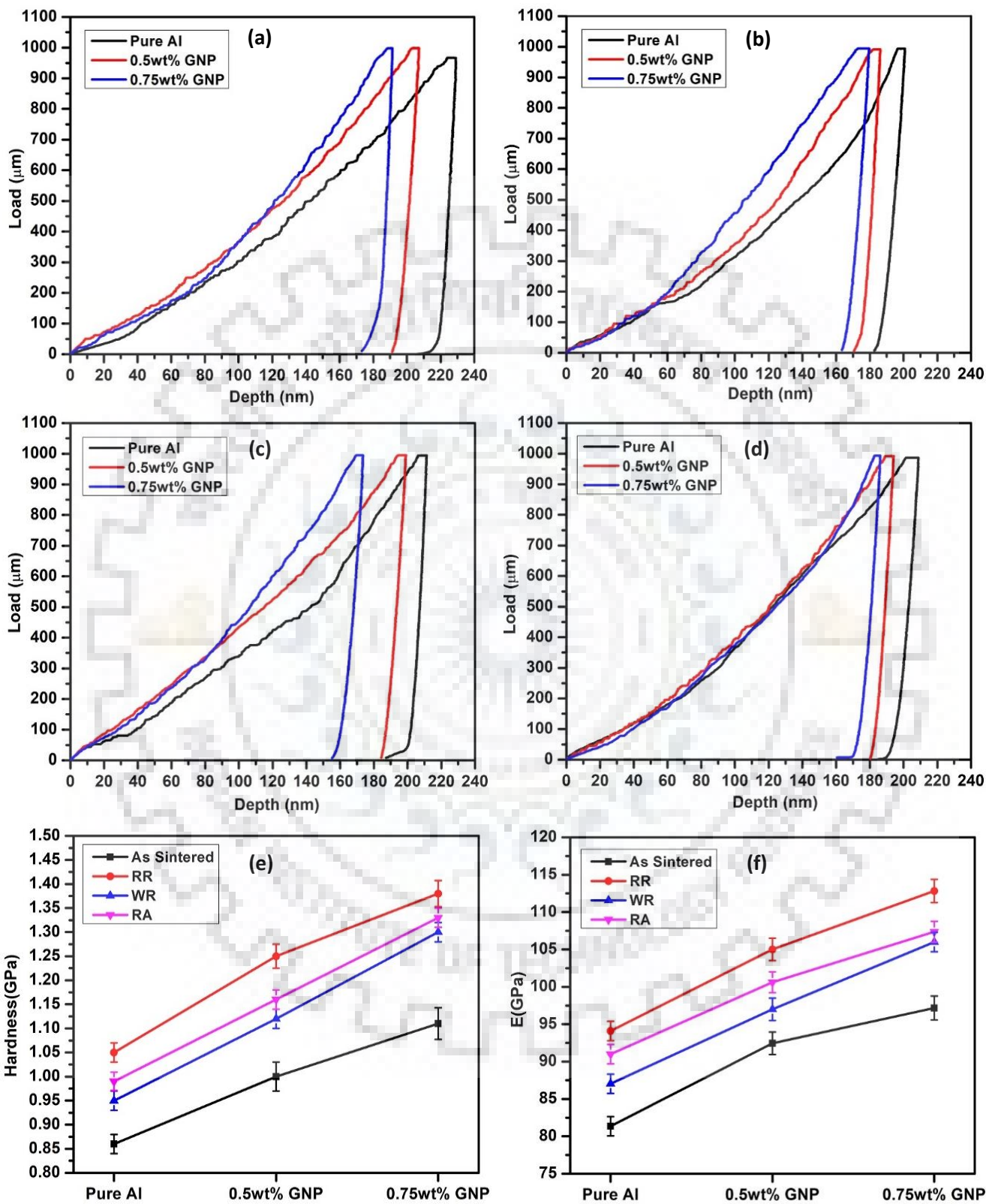
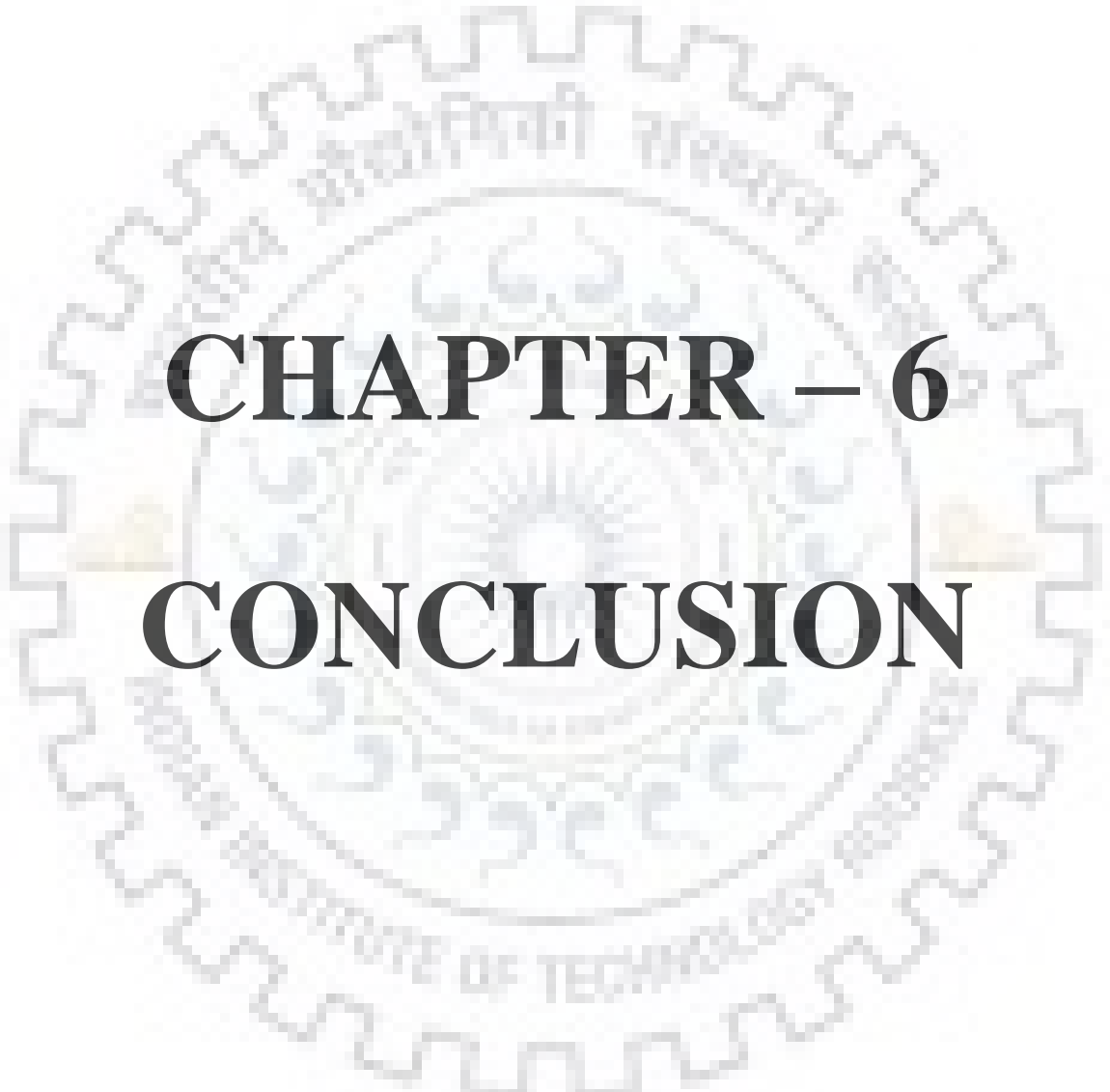


Fig.21 Representation of load vs. depth curve obtained from nanoindentation tests of (a) As-sintered, (b) RR, (c) WR, (d) RA; Variation in (e) hardness and (f) Elastic modulus

the failure strain of 0.75GNP/Al by 56.1% over 0.75GNP/Al RR (fig. 20(d)). This is due to grain size reduction, sub grain formation, delaying of failure by deflection of cracks; additionally, generation of dislocation due to raise of thermal strain mismatch between Al ( $\alpha_{CTE} = 23.6 \times 10^{-6} \text{ K}^{-1}$ ) [5] and GNP ( $\alpha_{CTE} = -8.0 \times 10^{-6} \text{ K}^{-1}$ ) [63]. There is an increment of ultimate tensile strength and yield strength of 0.75GNP/Al WR by 58.7% and 67.8% over pure Al WR. During annealing after rolling, as the residual stress is released, the region near the GNP is hindered to relieve this stress amounting in accumulation of dislocation at that province. Eventually, there is no significant change in ductility compared to WR. There is an improvement in the strength of 0.5 and 0.75GNP/Al by 24.4% and 54.5%, respectively, over pure Al RA. The ductility of 0.75GNP/Al RA is increased by 51.2% over 0.75GNP/Al RR.

Toughness calculated from area under stress-strain curve (fig. 20(c)) showed highest improvement by 0.5GNP/Al WR of 83.4% over 0.5GNP/Al RR, while 0.75GNP/Al WR improved by 42.4% over 0.75GNP/Al RR. It is observed (fig. 21(f)) that elastic modulus is enhanced with the content of GNP, signifying that strain hardening increases with increase in GNP[64]. In order to determine the elastic modulus and hardness of the samples, nano-indenter is used in quasi-static indentation mode. Fig. 21(a-d) shows the load vs. depth plot acquired from nano-indentation tests. With the increase in the GNP content, the depth of indent is decreasing, signifying the increment in the hardness. Hardness of 0.75GNP/Al RR is improved by 24.3% over 0.75GNP/Al as-sintered and 31.4% over pure Al. Comparatively, 0.75GNP/Al WR has 36.8% increment in hardness over pure Al WR. The increase in hardness seen in fig. 21(e) is considerably due to increase in dislocation density, contribution of reinforcement in load transfer and hence providing resistance to deformation. There is no significant difference in hardness and elastic modulus of WR and RA composites may be due to dynamic recovery and recrystallization occurring in both. Improvement by 13.6% and 19.4% in the elastic modulus of 0.5 and 0.75GNP/Al as-sintered composite is a result of high modulus of graphene. The elastic modulus increased by 22% for 0.75GNP/Al WR over pure Al WR showing less deformation of weak matrix at that temperature.





# **CHAPTER – 6**

# **CONCLUSION**

## 6. CONCLUSION

This study provides an understanding on the successful fabrication of GNP/Al composite through sintering by SPS technique. The effect of GNP, mechanical properties of GNP/Al composite, the effect of post treatment on it and microstructural behavior were analyzed. The main results of this work are concluded as: For as-sintered, it is observed that 0.75GNP/Al samples is giving better properties in terms of ultimate tensile strength, yield strength, hardness and elastic modulus. Despite of that, microvoids and cavities indicates that it is undesirable to increase the content of reinforcement after some extend which will lead to deterioration of the properties. The agglomeration of GNP due to van der waals force results in GNP-depleted region and poor interface, hindering the effective load transfer. The increase in dislocation density has further strengthened the composite material and enhanced the hardness when rolled at room temperature. Nevertheless, the intergranular fracture reflecting the brittleness resulted in low ductility. For WR, 0.5GNP/Al showed the highest toughness of  $1125 \text{ J/mm}^3$  that has significantly improved due to increase in failure strain upto 10%, which is attributed to deflection of cracks. 0.75wt% GNP/Al RA shows increment in tensile strength, hardness and elastic modulus by 55%, 34% and 18%, respectively compared to pure Al RA. Whereas, 0.75wt%GNP/Al WR showed the highest increment of UTM, YS, elastic modulus and hardness by 60%, 67%, 22% and 36%, respectively, compared to pure Al WR. The strength was retained due to thermal strain mismatch between matrix and reinforcement. Rolling followed by annealing showed combination of transgranular and intergranular fracture owing to the ductility of matrix and pinning effect of reinforcement as seen in warm rolling.

## LIST OF CONFERENCE PRESENTATION

Sr. No.	Conference Presentation details
1.	<b>Jijo ChristudasJustus, Ankita Bisht, Debrupa Lahiri.</b> “Mechanical Behavior of Aluminum-Graphene Composite as a Result of Thermo-Mechanical Treatment” 55 <sup>th</sup> National Metallurgists’ Day, <b>BITS Pilani Goa, India, 11<sup>th</sup>-14<sup>th</sup> Nov, 2017</b>
2.	<b>Jijo ChristudasJustus, Ankita Bisht, Debrupa Lahiri.</b> “Effect of Work Hardening and Annealing on Mechanical Behavior of Aluminum-Graphene Composite” Advances in Materials & Processing: Challenges & Opportunities (AMPCO 2017), <b>IIT Roorkee, Uttarakhand, India, 30<sup>th</sup> Nov- 2<sup>nd</sup> Dec, 2017</b>



## REFERENCES

- [1] J. L. Li, Y. C. Xiong, X. D. Wang, S. J. Yan, C. Yang, W. W. He, J. Z. Chen, S. Q. Wang, X. Y. Zhang, and S. L. Dai, “Microstructure and tensile properties of bulk nanostructured aluminum/graphene composites prepared via cryomilling,” *Materials Science and Engineering A*, vol. 626, pp. 400–405, 2015.
- [2] V. G. Konakov, O. Y. Kurapova, I. V. Lomakin, I. Y. Archakov, E. N. Solovyeva, and I. A. Ovid’ko, “FABRICATION OF ALUMINUM-GRAPHENE AND METAL-CERAMIC NANOCOMPOSITES. A SELECTIVE REVIEW,” vol. 44, pp. 361–369, 2016.
- [3] J. Wang, Z. Li, G. Fan, H. Pan, Z. Chen, and D. Zhang, “Reinforcement with graphene nanosheets in aluminum matrix composites,” *Scripta Materialia*, vol. 66, no. 8, pp. 594–597, 2012.
- [4] Sebastian Anthony (2013, August 27), “Graphene used to make graphene-copper composite that’s 500 times stronger | ExtremeTech.”, Retrieved from <https://www.extremetech.com/extreme/164961-graphene-used-to-make-graphene-copper-composite-thats-500-times-stronger>.
- [5] M. Rashad, F. Pan, A. Tang, and M. Asif, “Effect of Graphene Nanoplatelets addition on mechanical properties of pure aluminum using a semi-powder method,” *Progress in Natural Science: Materials International*, vol. 24, no. 2, pp. 101–108, 2014.
- [6] S. C. Tjong, “Recent progress in the development and properties of novel metal matrix nanocomposites reinforced with carbon nanotubes and graphene nanosheets,” *Materials Science and Engineering R: Reports*, vol. 74, no. 10, pp. 281–350, 2013.
- [7] B. W. Soutter, “Graphene Composite Materials Graphene Composites in Battery Electrodes,” pp. 1–5, 2013.

- [8] Y. Huang, Q. Ouyang, D. Zhang, J. Zhu, R. Li, and H. Yu, "Carbon materials reinforced aluminum composites: A review," *Acta Metallurgica Sinica (English Letters)*, vol. 27, no. 5, pp. 775–786, 2014.
- [9] S. Stankovich, D. A. Dikin, G. H. B. Dommett, K. M. Kohlhaas, E. J. Zimney, E. A. Stach, R. D. Piner, S. B. T. Nguyen, and R. S. Ruoff, "Graphene-based composite materials," *Nature*, vol. 442, no. 7100, pp. 282–286, 2006.
- [10] K. S. Novoselov, A. K. Geim, S. V. Morozov, D. Jiang, Y. Zhang, S. V. Dubonos, I. V. Grigorieva, and A. A. Firsov, "Electric field effect in atomically thin carbon films.," *Science*, vol. 306, no. 5696, pp. 666–669, 2004.
- [11] A. K. Geim, "Nobel Lecture: Random walk to graphene," *Reviews of Modern Physics*, vol. 83, no. 3, pp. 851–862, 2011.
- [12] A. K. Geim, "Graphene : Status and Prospects," *Science*, vol. 324, no. 2009, pp. 1530–1534, 2009.
- [13] V. Singh, D. Joung, L. Zhai, S. Das, S. I. Khondaker, and S. Seal, "Graphene based materials: Past, present and future," *Progress in Materials Science*, vol. 56, no. 8, pp. 1178–1271, 2011.
- [14] K. Spyrou and P. Rudolf, "An Introduction to Graphene," *Functionalization of Graphene*, pp. 1–20, 2014.
- [15] M. Skoda, I. Dudek, A. Jarosz, and D. Szukiewicz, "Graphene: One material, many possibilities - Application difficulties in biological systems," *Journal of Nanomaterials*, vol. 2014, 2014.
- [16] S. F. Bartolucci, J. Paras, M. A. Rafiee, J. Rafiee, S. Lee, D. Kapoor, and N. Koratkar, "Graphene-aluminum nanocomposites," *Materials Science and Engineering A*, vol. 528, no. 27, pp. 7933–7937, 2011.
- [17] M. Rashad, F. Pan, Z. Yu, M. Asif, H. Lin, and R. Pan, "Investigation on microstructural,

mechanical and electrochemical properties of aluminum composites reinforced with graphene nanoplatelets,” *Progress in Natural Science: Materials International*, vol. 25, no. 5, pp. 460–470, 2015.

- [18] P. Ashwath and M. Anthony Xavier, “The effect of ball milling & reinforcement percentage on sintered samples of aluminium alloy metal matrix composites,” *Procedia Engineering*, vol. 97, pp. 1027–1032, 2014.
- [19] S. J. Yan, S. L. Dai, X. Y. Zhang, C. Yang, Q. H. Hong, J. Z. Chen, and Z. M. Lin, “Investigating aluminum alloy reinforced by graphene nanoflakes,” *Materials Science and Engineering A*, vol. 612, pp. 440–444, 2014.
- [20] S. E. Shin and D. H. Bae, “Deformation behavior of aluminum alloy matrix composites reinforced with few-layer graphene,” *Composites Part A: Applied Science and Manufacturing*, vol. 78, pp. 42–47, 2015.
- [21] K. S. Reddy, D. Sreedhar, K. D. Kumar, and G. P. Kumar, “Role of Reduced Graphene Oxide on Mechanical-thermal Properties of Aluminum Metal Matrix Nano Composites,” *Materials Today: Proceedings*, vol. 2, no. 4–5, pp. 1270–1275, 2015.
- [22] Z. Li, Q. Guo., Z. Li, D. B. Xiong, Y. Su, J. Zhang, and D. Zhang, “Supporting information-Enhanced mechanical properties of graphene/aluminum composites,” *Nano Letters*, vol. 1, no. Zhang D, pp. 1–19, 2015.
- [23] S. E. Shin, H. J. Choi, J. H. Shin, and D. H. Bae, “Strengthening behavior of few-layered graphene/aluminum composites,” *Carbon*, vol. 82, no. C, pp. 143–151, 2015.
- [24] G. Li and B. Xiong, “Effects of graphene content on microstructures and tensile property of graphene-nanosheets / aluminum composites,” *Journal of Alloys and Compounds*, vol. 697, pp. 31–36, 2017.



- [25] J. Liu, Y. Yang, H. Hassanin, N. Jumbu, S. Deng, Q. Zuo, and K. Jiang, "Graphene – Alumina Nanocomposites with Improved Mechanical Properties for Biomedical Applications," *ACS Applied Materials & Interfaces*, vol. 8, pp. 2607–2616, 2016.
- [26] J. Kusui, K. Fujii, K. Yokoe, T. Yokota, K. Osamura, O. Kubota, and H. Okuda, "Development of Super-High Strength Al-Zn-Mg-Cu P/M Alloys," *Materials Science Forum*, vol. 217–222, pp. 1823–1828, 1996.
- [27] Q. Wang, Z. Zhao, Y. Zhao, K. Yan, C. Liu, and H. Zhang, "The strengthening mechanism of spray forming Al-Zn-Mg-Cu alloy by underwater friction stir welding," *Materials and Design*, vol. 102, pp. 91–99, 2016.
- [28] J. Dong, Z. Zhao, J. Cui, F. Yu, and C. Ban, "Effect of low-frequency electromagnetic casting on the castability, microstructure, and tensile properties of direct-chill cast Al-Zn-Mg-Cu alloy," *Metallurgical and Materials Transactions A*, vol. 35, no. August, pp. 2487–2494, 2004.
- [29] M. Shaarbaaf and M. R. Toroghinejad, "Nano-grained copper strip produced by accumulative roll bonding process," *Materials Science and Engineering A*, vol. 473, no. 1–2, pp. 28–33, 2008.
- [30] Y. H. Zhao, X. Z. Liao, Z. Jin, R. Z. Valiev, and Y. T. Zhu, "Microstructures and mechanical properties of ultrafine grained 7075 Al alloy processed by ECAP and their evolutions during annealing," *Acta Materialia*, vol. 52, no. 15, pp. 4589–4599, 2004.
- [31] M. Noda, M. Hirohashi, and K. Funami, "Low temperature superplasticity and its deformation mechanism in grain refinement of Al-Mg alloy by multi-axial alternative forging," *Nippon Kinzoku Gakkaishi/Journal of the Japan Institute of Metals*, vol. 67, no. 2, pp. 98–105, 2003.
- [32] D. C. C. Magalhães, M. F. Hupalo, and O. M. Cintho, "Natural aging behavior of AA7050 Al alloy after cryogenic rolling," *Materials Science and Engineering A*, vol. 593, pp. 1–7, 2014.
- [33] J. Adrien, E. Maire, R. Estevez, J. C. Ehrstrom, and T. Warner, "Influence of the

thermomechanical treatment on the microplastic behaviour of a wrought Al-Zn-Mg-Cu alloy,” *Acta Materialia*, vol. 52, no. 6, pp. 1653–1661, 2004.

- [34] J. Zuo, L. Hou, J. Shi, H. Cui, L. Zhuang, and J. Zhang, “Enhanced plasticity and corrosion resistance of high strength Al-Zn-Mg-Cu alloy processed by an improved thermomechanical processing,” *Journal of Alloys and Compounds*, vol. 716, pp. 220–230, 2017.
- [35] H. G. Prashantha Kumar and M. Anthony Xavier, “Graphene reinforced metal matrix composite (GRMMC): A review,” *Procedia Engineering*, vol. 97, pp. 1033–1040, 2014.
- [36] Y. Si and E. T. Samulski, “Exfoliated graphene separated by platinum nanoparticles,” *Chemistry of Materials*, vol. 20, no. 21, pp. 6792–6797, 2008.
- [37] C. Xu, X. Wang, and J. Zhu, “Graphene–Metal Particle Nanocomposites,” *The Journal of Physical Chemistry C*, vol. 112, no. 50, pp. 19841–19845, 2008.
- [38] B. Song, D. Li, W. Qi, M. Elstner, C. Fan, and H. Fang, “Graphene on Au(111): A highly conductive material with excellent adsorption properties for high-resolution bio/nanodetection and identification,” *ChemPhysChem*, vol. 11, no. 3, pp. 585–589, 2010.
- [39] J. Gong, T. Zhou, D. Song, and L. Zhang, “Monodispersed Au nanoparticles decorated graphene as an enhanced sensing platform for ultrasensitive stripping voltammetric detection of mercury(II),” *Sensors and Actuators, B: Chemical*, vol. 150, no. 2, pp. 491–497, 2010.
- [40] “ANSTO Publications Online\_ Enhanced reversible lithium storage in a nanosize silicon\_graphene composite.”
- [41] L. Y. Chen, H. Konishi, A. Fehrenbacher, C. Ma, J. Q. Xu, H. Choi, H. F. Xu, F. E. Pfefferkorn, and X. C. Li, “Novel nanoprocessing route for bulk graphene nanoplatelets reinforced metal matrix nanocomposites,” *Scripta Materialia*, vol. 67, no. 1, pp. 29–32, 2012.
- [42] C. L. P. Pavithra, B. V. Sarada, K. V. Rajulapati, T. N. Rao, and G. Sundararajan, “A new

electrochemical approach for the synthesis of copper-graphene nanocomposite foils with high hardness,” *Scientific Reports*, vol. 4, pp. 1–7, 2014.

- [43] W. Tian, S. Li, B. Wang, X. Chen, J. Liu, and M. Yu, “Graphene-reinforced aluminum matrix composites prepared by spark plasma sintering,” *International Journal of Minerals, Metallurgy, and Materials*, vol. 23, no. 6, pp. 723–729, 2016.
- [44] O. Sitdikov, T. Sakai, H. Miura, and C. Hama, “Temperature effect on fine-grained structure formation in high-strength Al alloy 7475 during hot severe deformation,” *Materials Science and Engineering A*, vol. 516, no. 1–2, pp. 180–188, 2009.
- [45] A. Bisht, M. Srivastava, R. M. Kumar, I. Lahiri, and D. Lahiri, “Strengthening mechanism in graphene nanoplatelets reinforced aluminum composite fabricated through spark plasma sintering,” *Materials Science and Engineering A*, vol. 695, no. March, pp. 20–28, 2017.
- [46] W. Yang, Q. Zhao, L. Xin, J. Qiao, J. Zou, P. Shao, Z. Yu, Q. Zhang, and G. Wu, “Microstructure and mechanical properties of graphene nanoplates reinforced pure Al matrix composites prepared by pressure infiltration method,” *Journal of Alloys and Compounds*, vol. 732, pp. 748–758, 2018.
- [47] M. Li, H. Gao, J. Liang, S. Gu, W. You, D. Shu, J. Wang, and B. Sun, “Microstructure evolution and properties of graphene nanoplatelets reinforced aluminum matrix composites,” *Materials Characterization*, vol. 140, no. November 2017, pp. 172–178, 2018.
- [48] Z. Hu, F. Chen, J. Xu, Q. Nian, D. Lin, C. Chen, X. Zhu, Y. Chen, and M. Zhang, “3D printing graphene-aluminum nanocomposites,” *Journal of Alloys and Compounds*, vol. 746, pp. 269–276, 2018.
- [49] J. Li, X. Zhang, and L. Geng, “Improving graphene distribution and mechanical properties of GNP/Al composites by cold drawing,” *Materials and Design*, vol. 144, pp. 159–168, 2018.

- [50] M. Gürbüz, M. Can Şenel, and E. Koç, “The effect of sintering time, temperature, and graphene addition on the hardness and microstructure of aluminum composites,” *Journal of Composite Materials*, vol. 52, no. 4, pp. 553–563, 2018.
- [51] G. Fan, H. Huang, Z. Tan, D. Xiong, Q. Guo, M. Naito, Z. Li, and D. Zhang, “Grain refinement and superplastic behavior of carbon nanotube reinforced aluminum alloy composite processed by cold rolling,” *Materials Science and Engineering A*, vol. 708, no. July, pp. 537–543, 2017.
- [52] A. A. Najimi and H. R. Shahverdi, “Microstructure and mechanical characterization of Al6061-CNT nanocomposites fabricated by spark plasma sintering,” *Materials Characterization*, vol. 133, no. June, pp. 44–53, 2017.
- [53] P. Hidalgo-Manrique, S. Yan, F. Lin, Q. Hong, I. A. Kinloch, X. Chen, R. J. Young, X. Zhang, and S. Dai, “Microstructure and mechanical behaviour of aluminium matrix composites reinforced with graphene oxide and carbon nanotubes,” *Journal of Materials Science*, vol. 52, no. 23, pp. 13466–13477, 2017.
- [54] E. Ghasali, P. Sangpour, A. Jam, H. Rajaei, K. Shirvanimoghaddam, and T. Ebadzadeh, “Microwave and spark plasma sintering of carbon nanotube and graphene reinforced aluminum matrix composite,” *Archives of Civil and Mechanical Engineering*, vol. 18, no. 4, pp. 1042–1054, 2018.
- [55] “Bulk Graphene Nanoplatelets | World-Leading Graphene Company - XG SciencesWorld-Leading Graphene Company – XG Sciences.” .
- [56] K. L. Yadav and P. K. Patel, “Bimodal distribution of grains,” *Materials Today*, vol. 19, no. 1, pp. 56–57, 2016.
- [57] K. H. Min, S. P. Kang, D. G. Kim, and Y. Do Kim, “Sintering characteristic of Al<sub>2</sub>O<sub>3</sub>-reinforced 2xxx series Al composite powders,” *Journal of Alloys and Compounds*, vol. 400, no.

1–2, pp. 150–153, 2005.

- [58] W. Zhao, D., Tie, “A precise method of calculating the parameter -the mean strain rate in rolling,” *Appl Sci*, vol. 13, no. 1995, p. 2018, 2018.
- [59] H. Li, W. Chen, L. Dong, Y. Shi, J. Liu, and Y. Q. Fu, “Interfacial bonding mechanism and annealing effect on Cu-Al joint produced by solid-liquid compound casting,” *Journal of Materials Processing Technology*, vol. 252, no. May 2017, pp. 795–803, 2018.
- [60] R. K. Roy, “Recrystallization Behavior of Commercial Purity Aluminium Alloys,” *World’s largest Science, Technology & Medicine Open Access book publisher*, pp. 79–98, 2016.
- [61] D. Schwartz, “NUCLEAR FORENSICS INTERNATIONAL TECHNICAL WORKING GROUP ITWG GUIDELINE ON POWDER X-RAY DIFFRACTION (XRD),” 2016.
- [62] S. R. Bakshi, D. Lahiri, and A. Agarwal, “Carbon nanotube reinforced metal matrix composites - a review,” *International Materials Reviews*, vol. 55, no. 1, pp. 41–64, 2010.
- [63] D. Yoon, Y. W. Son, and H. Cheong, “Negative thermal expansion coefficient of graphene measured by raman spectroscopy,” *Nano Letters*, vol. 11, no. 8, pp. 3227–3231, 2011.
- [64] D. Lahiri, S. R. Bakshi, A. K. Keshri, Y. Liu, and A. Agarwal, “Dual strengthening mechanisms induced by carbon nanotubes in roll bonded aluminum composites,” *Materials Science and Engineering A*, vol. 523, no. 1–2, pp. 263–270, 2009.